

OPEN ACCESS

**Repository of the Max Delbrück Center for Molecular Medicine (MDC)
in the Helmholtz Association**

<https://edoc.mdc-berlin.de/19091/>

SIX1 and SIX4 homeoproteins regulate PAX7+ progenitor cell properties during fetal epaxial myogenesis

Wurmser M., Chaverot N., Madani R., Sakai H., Negrone E., Demignon J., Saint-Pierre B., Mouly V., Amthor H., Tapscott S., Birchmeier C., Tajbakhsh S., Le Grand F., Sotiropoulos A., Maire P.

This is a copy of the final article, which is published here by [permission of the publisher](#) and which appeared first in:

Development
JJJJ MMM TT ; 147(19): dev185975
doi: [10.1242/dev.185975](https://doi.org/10.1242/dev.185975)

Publisher: [The Company of Biologists Ltd](#)

Copyright © 2020 The Authors. Published by The Company of Biologists Ltd.

SIX1 and SIX4 homeoproteins regulate PAX7+ progenitor cell properties during fetal epaxial myogenesis

Maud Wurmser¹, Nathalie Chaverot¹, Rouba Madani¹, Hiroshi Sakai^{2,3,4}, Elisa Negroni⁵, Josiane Demignon¹, Benjamin Saint-Pierre¹, Vincent Mouly⁵, Helge Amthor⁶, Stephen Tapscott⁷, Carmen Birchmeier⁸, Shahragim Tajbakhsh^{3,4}, Fabien Le Grand^{1,9}, Athanassia Sotiropoulos¹ and Pascal Maire^{1,*}

ABSTRACT

Pax7 expression marks stem cells in developing skeletal muscles and adult satellite cells during homeostasis and muscle regeneration. The genetic determinants that control the entrance into the myogenic program and the appearance of PAX7+ cells during embryogenesis are poorly understood. SIX homeoproteins are encoded by the sine oculis-related homeobox *Six1-Six6* genes in vertebrates. *Six1*, *Six2*, *Six4* and *Six5* are expressed in the muscle lineage. Here, we tested the hypothesis that *Six1* and *Six4* could participate in the genesis of myogenic stem cells. We show that fewer PAX7+ cells occupy a satellite cell position between the myofiber and its associated basal lamina in *Six1* and *Six4* knockout mice (s1s4KO) at E18. However, PAX7+ cells are detected in remaining muscle masses present in the epaxial region of the double mutant embryos and are able to divide and contribute to muscle growth. To further characterize the properties of s1s4KO PAX7+ cells, we analyzed their transcriptome and tested their properties after transplantation in adult regenerating tibialis anterior muscle. Mutant stem cells contribute to hypotrophic myofibers that are not innervated but retain the ability to self-renew.

KEY WORDS: Pax7, Six1, Six4, Homing, Stem cells, Myogenesis

INTRODUCTION

Muscle development in mouse takes place from embryonic day (E) 8 when the first *Myf5* expressing cells are detected in somites, and ends at the adult stage when muscle masses stop growing during homeostasis. Sequential waves of myogenesis build the hundreds of individual muscles characteristic of mammals. Primary myogenesis operates until E14, creating a scaffold of the distinct muscle groups (Duxson et al., 1989; Kelly and Zacks, 1969) with their specific spiral, spindle-like or triangular shapes. During this period, and depending on the embryonic region of the embryo (limb, dorsal axis), myogenic progenitors expressing the PAX3 homeopaired protein turn on the expression of myogenic regulatory factors

(MRFs). Committed and uncommitted myogenic cells are able to divide and to expand. MRF+ cells then activate myogenin (*Myog*) expression, differentiate and fuse to give rise to multinucleated primary myofibers (reviewed by Buckingham and Vincent, 2009; Comai and Tajbakhsh, 2014). From E11.5-E12, the bulk of the PAX3+/PAX7+ progenitors in the trunk arise from the central dermomyotome (DM), but before that, the dorsomedial (DML) and ventrolateral (VLL) lips release progenitors for epaxial and hypaxial muscles. Although lineage tracing has not yet been done in detail, epaxial PAX7+ cells appear to originate from all lips of the dermomyotome of the somite, including at later stages from the central DM. From E14, at the limb bud level, most undifferentiated PAX3+ cells downregulate this gene and retain *Pax7* expression after primary myogenesis. PAX7+ cells are also mitotically active, intermingle between the scaffold of primary myofibers, and progress towards MRF expression and cell fusion, thereby generating the second wave of secondary or fetal myofiber formation, arising from about E14 to birth (Buckingham and Vincent, 2009; Comai and Tajbakhsh, 2014). The balance between differentiation and self-renewal is finely regulated to allow harmonious growth without depletion of the myogenic stem cell pool. Deficits in secondary myogenesis are associated with muscle hypoplasia, as the number of myofibers increase significantly between E14 and birth in all muscle groups (reviewed by Biressi et al., 2007; Buckingham and Relaix, 2015; Comai and Tajbakhsh, 2014). During fetal development, several signaling pathways modulate the behavior of PAX7+ cells, among them BMP that promotes PAX7+ cell proliferation (Nord et al., 2013; Wang et al., 2010) and NOTCH that suppresses premature myogenic cell differentiation (Esteves de Lima et al., 2016; Mourikis et al., 2012a; Schuster-Gossler et al., 2007; Vasyutina et al., 2007). Although WNT/ β -catenin has been shown to promote the acquisition of a differentiated phenotype by both embryonic (Borello et al., 2006; Gros et al., 2009) and adult (Rudolf et al., 2016) muscle progenitor cells, it has also been proposed to amplify the population of PAX7+ cells in fetal/postnatal limb muscles (Hutcheson et al., 2009). Fetal muscle development is not profoundly altered in the absence of *Pax7* (Seale et al., 2000). However, ablation of PAX7+ cells during embryogenesis revealed impaired fetal muscle growth, indicating that PAX7+ cells are responsible for fetal muscle growth (Hutcheson et al., 2009; Lepper and Fan, 2010; Schienda et al., 2006).

Satellite cells (SCs) are muscle stem cells responsible for adult skeletal muscle regeneration (reviewed by Yin et al., 2013). These cells derive from PAX7+ progenitor cells responsible for skeletal muscle growth during fetal and postnatal myogenesis (Gros et al., 2005; Lepper and Fan, 2010; Seale et al., 2000). They require NOTCH signaling for efficient homing into their niche in the mouse fetus (Bröhl et al., 2012), and to maintain their progenitor properties

¹Université de Paris, Institut Cochin, INSERM, CNRS, 24 rue du Fg St Jacques, F-75014 Paris, France. ²Division of Integrative Pathophysiology, Proteo-Science Center, Ehime University, Toon, Ehime, 791-0295, Japan. ³Stem Cells and Development, Department of Developmental and Stem Cell Biology, Institut Pasteur, 25 rue du Dr. Roux, 75015, Paris, France. ⁴CNRS UMR 3738, Institut Pasteur, 75015 Paris, France. ⁵Sorbonne Université, Institut de Myologie, INSERM, 75013 Paris, France. ⁶INSERM U1179, LIA BAHN CSM, Université de Versailles Saint-Quentin-en-Yvelines, Montigny-le-Bretonneux, France. ⁷Fred Hutchinson Cancer Research Center, Seattle, USA. ⁸Max Delbrück Center for Molecular Medicine, Berlin, Germany. ⁹Institut NeuroMyoGène, Université Claude Bernard Lyon 1, CNRS, INSERM, 69008 Lyon, France.

*Author for correspondence (pascal.maire@inserm.fr)

 H.S., 0000-0001-9456-0911; P.M., 0000-0001-7795-0029

Handling Editor: Benoît Bruneau
Received 8 November 2019; Accepted 18 June 2020

and their pool in adulthood (Bjornson et al., 2012; Esteves de Lima et al., 2016; Mourikis et al., 2012b). Thus, adult SCs are located in a specialized microenvironment, the ‘satellite cell niche’, between the plasmalemma of differentiated myofibers and the basal lamina surrounding them (Mauro, 1961) allowing them to maintain their stemness (reviewed by Evano and Tajbakhsh, 2018). The positioning of SCs in this niche occurs during fetal myogenesis, and the majority of the PAX7⁺ cells are located under the basal lamina at birth (Bröhl et al., 2012; Relaix et al., 2005; Kassar-Duchossoy et al., 2015). During postnatal muscle growth, the number of myofibers in the mouse does not increase, and further growth is mainly due to myofiber hypertrophy (Ontell and Kozeka, 1984; White et al., 2010) dependent on SC nuclei accretion to growing myofibers until puberty and increased protein synthesis afterwards (Kim et al., 2016). Nuclei from SCs are also accreted to growing myofibers during adult muscle hypertrophy, and are required for this hypertrophy (Fukada et al., 2020; Guerci et al., 2012). Ablation of PAX7⁺ cells in adult muscle has clearly demonstrated their requirement for muscle regeneration during acute muscle injury (Lepper et al., 2011; Murphy et al., 2011; Sambasivan et al., 2011).

Extracellular matrix (ECM) that surrounds SCs, constituting their niche, participates in SC behavior. It is mainly composed of laminin (basal lamina), fibronectin (reticular lamina) and collagen VI (bounding the basal and reticular laminas) (Thomas et al., 2015) produced by PAX7⁺ cells, myofibers and by the cells of the microenvironment including fibroblasts and endothelial cells (Baghdadi et al., 2018; Bentzinger et al., 2013; Rayagiri et al., 2018; Urciuolo et al., 2013; Verma et al., 2018). How ECM progressively forms during fetal development, and which cell types participate in ECM formation leading to the homing of PAX7⁺ cells between the myofiber and the basal lamina, remains unclear. However, fetal PAX7⁺ cells secrete ECM proteins that participate in the remodeling of their microenvironment (Bentzinger et al., 2012; Bröhl et al., 2012; Rosen et al., 1992; Tierney and Sacco, 2016). Furthermore, formation of this ECM is also important to control proliferation of PAX7⁺ cells, as it polarizes the stem cells and influences their division axis (Feige et al., 2018).

Although the timing of PAX7⁺ cell homing into their niche has been described, several cellular and molecular cues involved in this process remain to be identified. The six sine oculis-related homeobox (*Six*) genes encode for the transcription factors SIX1 to SIX6 in vertebrates. *Six1* and *Six4* expression patterns are very similar during embryogenesis, and their proteins bind to the same DNA sequence, a property they also share with *Six2* and *Six5* (Chakroun et al., 2015; Kawakami et al., 1996; Relaix et al., 2013; Santolini et al., 2016). Consequently, *Six1 Six4* double knock-out (*s1s4KO*) mutants have a stronger myogenic phenotype than the simple mutants (Grifone et al., 2005; Laclef et al., 2003a; Ozaki et al., 2001). Indeed, *s1s4KO* mice display no hypaxial musculature, but back and craniofacial muscles, although reduced in size, are formed in these mutants (Grifone et al., 2005). Both *Six1* and *Six4* are expressed in adult SCs and have been implicated in muscle regeneration (Chakroun et al., 2015; Le Grand et al., 2012).

Here, we analyzed the genesis and properties of PAX7⁺ myogenic stem cells in wild-type (WT) and *s1s4KO* fetuses and observed that the absence of *Six1* and *Six4* does not affect PAX7⁺ cell emergence in remaining epaxial muscles but impairs their homing at the end of fetal development. Identification of the downstream targets of *Six1* and *Six4* revealed many genes coding for ECM proteins that are misregulated in mutant cells

that may participate in their defective properties. Finally, examination of *s1s4KO* PAX7⁺ cells by transplantation in adult regenerating limb muscle exposed deficits in muscle reconstruction.

RESULTS

SIX homeoproteins are expressed in a subpopulation of PAX7⁺ cells during fetal myogenesis

We and others have previously reported that Six genes are expressed in myogenic territories during embryonic and fetal development, in adult muscle fibers (Laclef et al., 2003a; Maire et al., 2020; Oliver et al., 1995; Relaix et al., 2013) and in their associated SCs, in which *Six1*, *Six4* and *Six5* mRNAs and proteins have been detected (Chakroun et al., 2015; Le Grand et al., 2012; Liu et al., 2013; Sakakibara et al., 2016; Yajima and Kawakami, 2016; Yajima et al., 2010). To analyze the dynamic expression of SIX1 in the PAX7⁺ population during fetal myogenesis, we performed co-immunostaining with SIX1 and PAX7 antibodies. At the epaxial level, we observed that half of the PAX7⁺ cell population expressed SIX1 from E14.5-E18.5 during fetal myogenesis (Fig. 1A,B), suggesting a persisting expression of *Six1* in myogenic progenitor cells. Myogenic PAX7⁺ cells can be subdivided into two main populations according either to *Pax7-nGFP* expression level – a *Pax7^{nGFP}high* and a *Pax7^{nGFP}low* population that differed in their properties (Rocheteau et al., 2012) – or according to MYF5 expression level that distinguishes a major fast-cycling PAX7+MYF5⁺ and a minor low-cycling PAX7+MYF5[−] population during embryogenesis (Picard and Marcelle, 2013). We investigated whether the PAX7+SIX1⁺ and PAX7+SIX1[−] cells had the same proliferation or differentiation potential. We observed that ~70% of PAX7⁺ cells were KI67⁺ (also known as MKI67) independently of SIX1 expression (35% were PAX7+SIX1+KI67⁺ and 32% were PAX7+SIX1−KI67⁺), but that almost all PAX7⁺ cells were MYOG[−] independently of SIX1 expression (Fig. 1C-F). Thus, *Six1* expression was active and restricted to a sub-population of PAX7⁺ cells during fetal myogenesis with no apparent impact on the relative proliferation or differentiation of fetal PAX7⁺ cells, suggesting that it is not specifically involved in the control of the fast- or low-cycling PAX7⁺ cells.

SIX1 and SIX4 proteins are required for PAX7⁺ cell homing during fetal myogenesis

We first tested whether the absence of both *Six1* and *Six4* could modify the behavior of the PAX7⁺ cell population. We were unable to detect PAX7⁺ cells in the limbs of E18.5 mutant fetuses (Fig. S1), in agreement with the absence of hypaxial muscles, including limb muscles, in this mutant (Grifone et al., 2005). SIX1 and SIX4 proteins were therefore required for the emergence of PAX7⁺ hypaxial cells at the limbs level.

We observed no alteration in the number of PAX7⁺ cells/μm² in the residual back muscles at E14.5 or E18.5 (Fig. 2A,B). Interestingly, we found significantly more PAX7⁺ in the interstitial space, outside of the basal lamina of *s1s4KO* back muscles compared with the WT at E18.5, suggesting homing defects (Fig. 2A,C). Notably, the homing process of PAX7⁺ cells from the interstitial space to their niche – between the myofiber plasma membrane and the basal lamina – takes place during mouse embryogenesis, between E14.5 and birth (Bröhl et al., 2012; Gros et al., 2005; Kassar-Duchossoy et al., 2005; Relaix et al., 2005), as shown in Fig. 2 in WT fetuses. To test the hypothesis that *Six1* and *Six4* genes could participate in this process, we compared the location of fetal PAX7⁺ cells relative to the ECM. In E14.5 WT

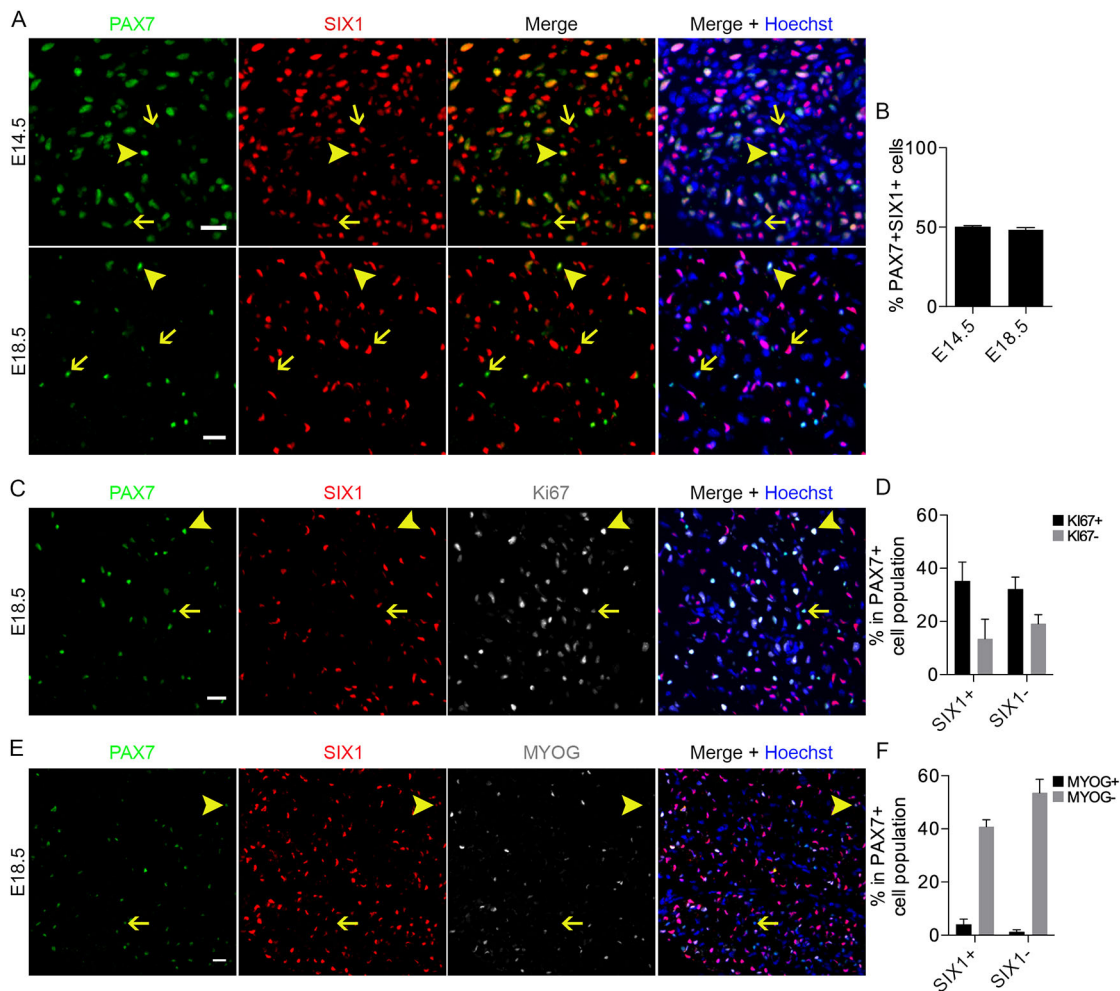


Fig. 1. SIX1 is expressed in the PAX7+ cell population during fetal myogenesis. (A,C,E) Transverse sections of immunostaining on E14.5 and E18.5 WT fetuses showing epaxial back muscle erector spinae. On all images nuclei are stained with Hoechst (blue). A shows immunostaining for PAX7 (green) and SIX1 (red). Arrows point to either PAX7+SIX1- or PAX7-SIX1+ cells, arrowheads to PAX7+SIX1+ cells. C shows immunostaining for PAX7 (green), SIX1 (red) and Ki67 (white). Arrows point to a PAX7+SIX1+Ki67+ cell and arrowheads to a PAX7+SIX1-Ki67- cell. E shows immunostaining for PAX7 (green), SIX1 (red) and MYOG (white). Arrows point to a PAX7+SIX1+MYOG- cell and arrowheads to a PAX7+SIX1-MYOG+ cell. (B) Quantification of the percentage of PAX7+SIX1+ cells among the whole PAX7+ cell population (E14.5 $n=2$, E18.5 $n=4$). (D) Quantification of the percentage of PAX7+ cells that are Ki67+ or Ki67- in the SIX1+ or SIX1- group of cells ($n=3$). (F) Quantification of the percentage of PAX7+ cells that are MYOG+ or MYOG- in the SIX1+ or SIX1- group of cells ($n=2$). An average of 300-500 PAX7+ cells have been counted per embryo. Data are mean \pm s.d. Scale bars: 20 μ m.

fetuses, we observed that all primary myofibers organized as groups [detected by MF20 immunostaining against sarcomeric MYH (myosin heavy chain)] were surrounded by laminin and collagen VI, and that fibronectin puncta start to organize around them (Fig. S2). Furthermore, all PAX7+ cells were located in the interstitial space: we detected no PAX7+ cells in contact with primary myofibers at that stage. At E16.5, we observed that 60% of PAX7+ cells were localized under the basal lamina of myofibers in WT muscles and that interstitial PAX7+ cells were located between the basal and the reticular lamina (Fig. 2A,C, Fig. S2), while some of them appeared in between basal lamina layers (Fig. S2). In E18.5 WT fetuses less than 20% of PAX7+ cells remained in the interstitial space and most PAX7+ cells were located under the basal lamina and the reticular lamina surrounding it (Fig. 2A,C, Fig. S2). Thus, PAX7+ cell homing is a dynamic and gradual process during fetal muscle growth.

In s1s4KO fetuses, we also observed a gradual homing of PAX7+ cells between E14.5 and E18.5. However, more than 55% of the PAX7+ cells remained in the interstitial space at E18.5 (Fig. 2A,C), suggesting a delay in the homing process. Of note, we observed no

defect of PAX7+ cell homing in remaining back and limb muscles of E18.5 s1KO and s5KO fetuses (Fig. S3). Importantly, PAX7+ cell homing was not further altered by additional lack of *Six5* in back muscles in s1s4s5 triple-KO fetuses, indicating that the homing phenotype was specific to the s1s4KO genotype (Fig. S3).

Impaired homing of PAX7+ cells in s1s4KO epaxial muscle is not linked to proliferation or differentiation defects

To determine whether PAX7+ cell location was associated with changes in proliferation or differentiation, we analyzed PAX7+Ki67+, PAX7+BrdU+ and MYOG+ cells in WT and s1s4KO fetuses. At E18.5, we found similar numbers of proliferating PAX7+ cells in WT and s1s4KO muscles, both in the niche and interstitial space, indicating that proliferation of PAX7+ s1s4KO cells was not compromised by homing deficiency (Fig. S4A-C). We observed no major modification in the number of MYOG+/ μ m² cells in back muscles between E14.5 and E18.5 WT and s1s4KO fetuses, and MYOG+ cell location regarding to the basal lamina was similar (Fig. S4D,E). Indeed, in WT and s1s4KO conditions, 20% of MYOG+ cells were located in the interstitial

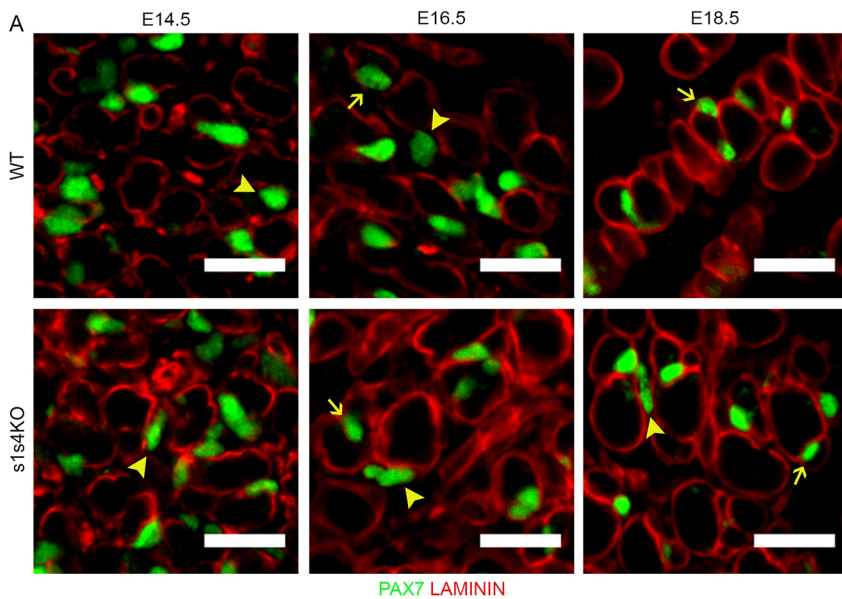


Fig. 2. *Six1* and *Six4* are required for PAX7+ cell homing during fetal myogenesis. (A) Immunostainings for PAX7 (green) and laminin (red) on E14.5, E16.5 and E18.5 WT and s1s4KO fetus transverse sections, showing the back muscle erector spinae. Arrows point to PAX7+ cells located under the basal lamina, arrowheads to PAX7+ cells located in the interstitial space. (B) Quantification of the number of PAX7+ cells/μm² (E14.5 WT *n*=4, E14.5 s1s4KO *n*=2, E18.5 WT *n*=2, E18.5 WT *n*=3). (C) Quantification of the percentage of interstitial PAX7+ cells (E14.5 *n*=3, E16.5 *n*=3, E18.5 *n*=6). ***P*<0.01, *****P*<0.0001. Data are mean±s.d. Scale bars: 20 μm.

space at E14.5, whereas 80% were located under the basal lamina. This indicated that, at E14.5, most myogenic cells differentiated under the basal lamina, where PAX7+ cells were absent, probably reflecting fusion of MYOG+PAX7− myogenic cells with pre-existing primary myofibers. At E18.5, only 10% of MYOG+ cells were located in the interstitial space, in agreement with the gradual homing of PAX7+ cells (Fig. S4). These data suggest that SIX1 and SIX4 homeoproteins are required for proper homing of fetal PAX7+ cells and that the impairment of PAX7+ cell location observed in s1s4KO did not affect their proliferation nor myogenic differentiation.

Six1* and *Six4* are dispensable for PAX7+ cell motility but required for their fusion *in vitro

To better understand the behavior of E18.5 s1s4KO PAX7+ cells, we analyzed their properties *ex vivo*. PAX7-nGFP positive cells were isolated by fluorescence-activated cell sorting (FACS) from WT and s1s4KO E18.5 fetuses and cultured on Matrigel. No difference was detected in the percentage of Ki67+, BrdU+ or PH3+ cells between WT and s1s4KO cells in proliferation medium (PM), confirming our *in vivo* data (Fig. 3A,B). Examination by video microscopy of WT and s1s4KO primary PAX7+ cells in PM for 6 h did not reveal any major cell motility defects (Fig. S5A). As SIX homeoproteins are known to control MRF expression, we compared the behavior of WT and s1s4KO primary PAX7+ cells following culture in differentiation medium (DM) for 3 days. We noted that most differentiated WT nuclei were located in more than two nuclei-containing MYH+ cells, whereas most differentiated s1s4KO nuclei are found in mononucleated MYH+ cells (Fig. 3C,D). This suggested that s1s4KO cells could differentiate (as they similarly

express MYH), but they were deficient in fusion. Examination of regulators of cell fusion showed that myomixer (*Mymx*) expression was blunted in mutant cells, whereas the expression of myomaker (*Mymk*) was not significantly altered (Fig. 3E). We also tested the capacity of WT and s1s4KO cells to generate reserve cells in DM. Although the percentage of PAX7+ nuclei after 3 days in DM was similar between WT and s1s4KO cultures, the proportion of PAX7+MYOG− cells among all MYH− mononucleated cells was slightly reduced. The proportion of PAX7−MYOG− was not significantly increased in s1s4KO cultures compared with WT (Fig. 3F), suggesting that SIX1 and SIX4 did not alter *Pax7* expression nor the stemness properties of myogenic cells. Analysis of adult PAX7+ cells from the single *Six1* mutant also revealed fusion index deficiency and no alteration of *Pax7* gene expression *ex vivo* (Le Grand et al., 2012).

The fact that *Six1* and *Six4* control cell metabolism in adult myofibers (Meng et al., 2013; Sakakibara et al., 2016) and in cancer cells (Li et al., 2018), and that metabolism modulates myogenic stem cells properties (Ryall, 2013; Theret et al., 2017), prompted us to conduct analysis of cellular bioenergetics and quantification of intracellular ATP concentration. However, WT and s1s4KO cells showed no major difference in mitochondrial oxidative activity nor in maximal respiratory capacity (Fig. S5B,C).

Genes coding for ECM and secreted proteins are misregulated in PAX7-nGFP+ cells in s1s4KO fetuses

To assess how *Six1* and *Six4* modulate PAX7+ cells properties and their homing, we performed a transcriptomic analysis by generating microarray data of PAX7-nGFP+ cells or whole back muscle from WT and s1s4KO fetuses at E15.5, when homing initiates, and at

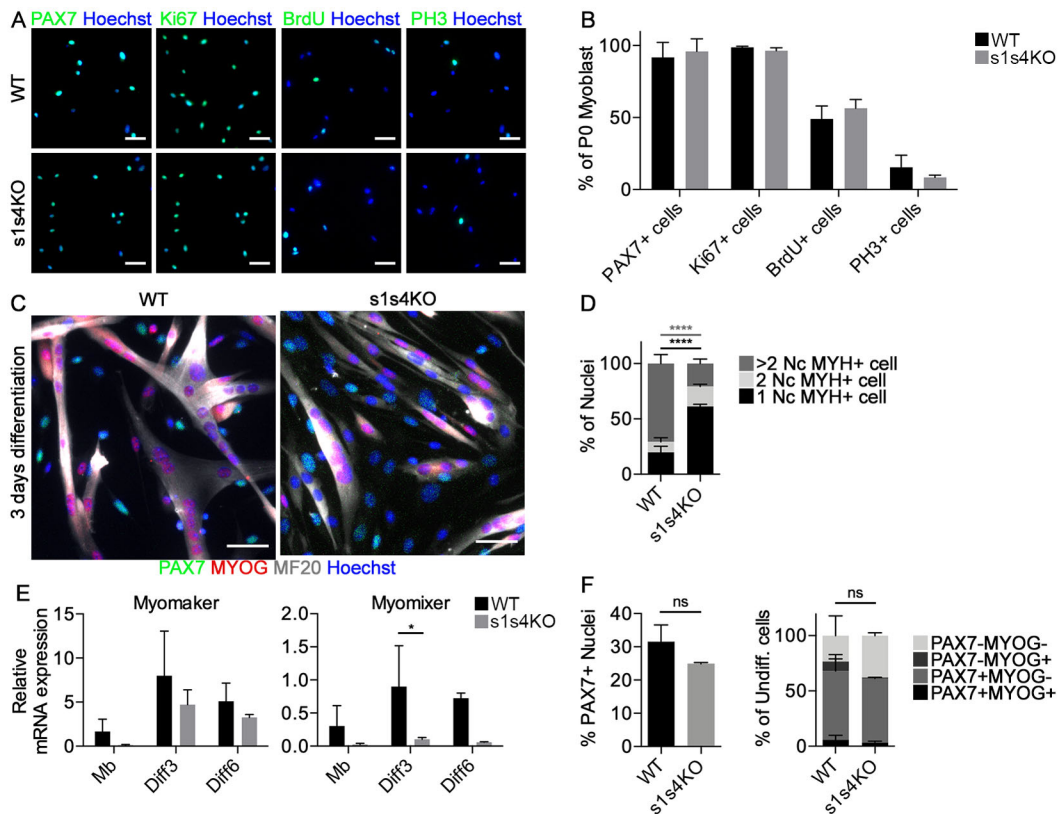


Fig. 3. Absence of *Six1* and *Six4* impairs myoblast fusion *in vitro*. (A) Immunostaining for PAX7, Ki67, BrdU and Phospho-Histone H3 (PH3) on freshly isolated (P0) WT (upper panels) and s1s4KO (lower panels) myoblasts cultivated in PM. (B) Quantification of the percentage of proliferating PAX7+, Ki67+, BrdU+ or PH3+ WT and s1s4KO myoblasts ($n=3-5$). (C) Immunostaining for PAX7 (green), MYOG (red) and MF20 (gray) on WT and s1s4KO cells after 3 days in DM. (D) Quantification of the percentage of nuclei in MYH+ cells containing 1 nucleus, 2 or >2 nuclei in WT and s1s4KO culture after 3 days in DM ($n=2-4$). (E) Relative mRNA expression of myomaker and myomixer gene in myoblasts in PM (Mb) and after 3 and 6 days in DM (Diff3, Diff6) of WT and s1s4KO cells ($n=2-4$). (F) Quantification of the percentage of reserve PAX7+ cells ($n=2-4$) (left), and percentage of PAX7 \pm MYOG \pm mononucleated cells among the MYH- cells (right) in WT and s1s4KO culture after 3 days in DM ($n=2-4$). An average of 500-1500 nuclei have been counted per n . * $P<0.05$, **** $P<0.0001$. ns, not significant. Data are mean \pm s.d. Scale bars: 50 μ m.

E18.5. The expression level of some candidate genes was then validated by quantitative reverse transcription PCR (RT-qPCR) (Fig. 4A, Fig. S7A, Tables S11, S12).

In agreement with our PAX7 and MYOG immunostaining data (Fig. 1) the expression levels of *Pax3*, *Pax7*, *Myf5*, *MyoD* and *Myog* was not modified in the microarray data of s1s4KO PAX7-nGFP+ cells. We also observed that *Six2* and *Six5* were expressed in myogenic cells at both stages of development, and that the absence of *Six1* and *Six4* was not compensated for by their upregulation. We validated these data by RT-qPCR experiments (Fig. S6). Microarray data were analyzed by comparing the expression of genes between WT and s1s4KO samples at E15.5 or E18.5 (using a fold change >2 or <2, and a P -value<0.05 as a cutoff), in PAX7-nGFP+ cells (Fig. 4A-E, Fig. S7B,C, Tables S1-S4) and in the whole back muscles (Fig. S7D,E, Tables S5-S8).

We studied the dynamics of gene expression from E15.5 to E18.5 in both WT and s1s4KO PAX7-nGFP+. Genes coding for ECM proteins (*Hmgn2*, *Fbln5*, *Mgp*), receptors and ligands involved in cellular guidance (*Gfra2*, *Chrdl2*, *Cntm6*, *Il17ra*, *Dpt*), and ECM degrading proteins (*Mmp2*) were upregulated in WT PAX7-nGFP+ cells between E15.5 and E18.5, and we did not observe this upregulation in s1s4KO cells. These results were also confirmed by RT-qPCR (Figs 4F and 5). The increased expression of all those genes over time might be essential for the establishment of PAX7+ cell environment and their mis-expression in s1s4KO cells could

account for their homing defect. Interestingly, genes coding for adhesion molecules (*Ninj1*, *Itga4*) were downregulated in WT PAX7-nGFP+ cells between E15.5 and E18.5, whereas their expression was not changed in s1s4KO cells (Fig. 4D,G). Although mildly affected, the expression of other ECM protein coding genes (*Tnc*, *Lama4*, *Lamb2*, *Lamc1*, *Fn1*, *Col6a2*, *Col6a6*) was downregulated in mutant PAX7-nGFP+ cells at E18.5 (Table S11).

Analyzing independently E15.5 and E18.5 stages, we observed that genes of the BMP/TGF β pathway were downregulated in s1s4KO PAX7-nGFP+ cells at E15.5 (*Bmp7*, *Mstn*) or E18.5 (*Chrdl2*, *Bmp4*, *Ltbp1* and *Tgfb3*) (Fig. 4E, Table S9). Altogether, the decreased expression of many ECM genes by mutant PAX7+ cells may participate in their homing process deficiency.

Genes coding for ECM and secreted proteins are misregulated in whole back muscles of s1s4KO fetuses

The absence of expression of SIX1 and SIX4 proteins in back muscle fibers could also explain the homing defect of s1s4KO PAX7+ cells. Therefore, we studied gene expression at E15.5 and E18.5 in both WT and s1s4KO back muscle masses. Genes related to calcium homeostasis (*Casq1*, *Atp2a1*, *Myoz1*) were downregulated in mutant muscles at both stages. On the other hand, genes coding for ECM proteins or secreted signaling proteins (*Tnc*, *Sema3D*, *Slit2*, *Sfrp1*, *Cxcl14*, *Rspo3*) and repulsive molecules (*Efna3*, *Efna2*, *Efnb2*, *Efna4* and *Efnb3*) known to

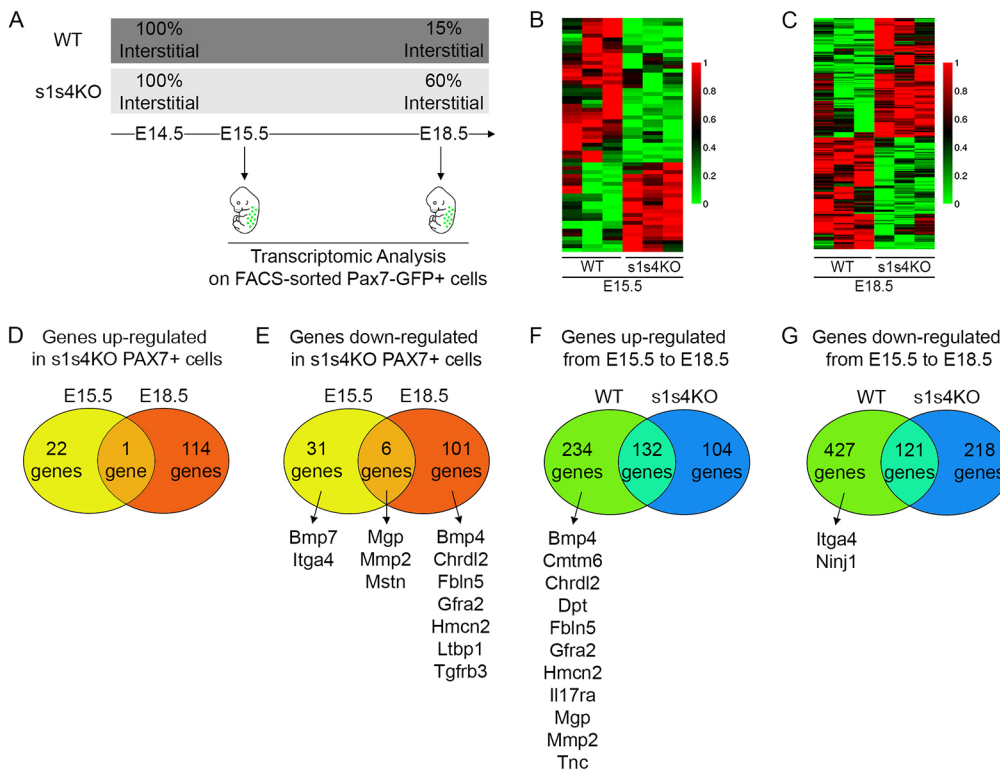


Fig. 4. Transcriptomic analysis of WT and s1s4KO PAX7+ cells.

(A) Affymetrix analysis has been performed from RNA extracted from FACS-sorted PAX7+ cells of WT and s1s4KO E15.5 and E18.5 fetus back muscles. (B) Heatmap representing up- and downregulated genes between WT and s1s4KO PAX7+ cells at E15.5. (C) Heatmap representing up- and downregulated genes between WT and s1s4KO PAX7+ cells at E18.5. (D,E) Venn diagrams representing upregulated (D) and downregulated (E) genes in s1s4KO PAX7+ cells compared with WT PAX7+ cells at E15.5 and E18.5. (F,G) Venn diagrams representing upregulated (F) and downregulated (G) genes at E18.5 compared with E15.5 WT and s1s4KO PAX7+ cells.

restrict myogenic cells contacts (Stark et al., 2011) were upregulated in mutant muscles at E15.5 (Fig. S7D, Table S10).

Altogether, our data show that s1s4KO PAX7+ cells and back muscles were defective in formation of the niche during fetal development, and that many genes were differentially regulated in PAX7+ cells and total muscles during WT fetal myogenesis between E15.5 and E18.5, a time when PAX7+ cells acquired a niche position.

ECM proteins known to participate in the myogenic stem cell niche are deficient in mutant PAX7+ cells

We further compared our Affymetrix transcriptomic data with a study reporting homing deficiency of PAX3+ cells with altered NOTCH and MYOD signaling pathways (Bröhl et al., 2012). Among the genes misregulated in E17.5 mutant *RBPJ^{lox/lox};Pax3^{CRE/+};MyoD^{-/-}* PAX3+ cells, we identified three genes that were upregulated between E15.5 and E18.5 in WT PAX7-nGFP+ cells (*Dag1*, *Chodl* and *Hmcn2*) (Table S11) and three genes that were both down-regulated in *RBPJ^{lox/lox};Pax3^{CRE/+};MyoD^{-/-}* PAX3+ cells and in s1s4KO PAX7+ cells (*Hmcn2*, *Lrrn1* and *Msc*), showing that other pathways than the NOTCH pathway were deficient in s1s4KO PAX7+ cells and responsible for the homing deficit observed.

Finally, we compared our data with a gene set enrichment analysis (GSEA) that characterized genes specifically expressed in fetal (E16.5) compared with adult activated (2-month-old) PAX7+ cells (Tierney and Sacco, 2016). We observed that some of the fetal genes, elastin, *Coll5a1*, fibrillin 1, *Col5a1*, *Coll2a1*, matrilin 2 and *Tnc*, were more strongly upregulated between E15.5 and E18.5 in WT PAX7-nGFP+ cells than in s1s4KO PAX7-nGFP+ cells (Tables S9 and S11), suggesting a maturation delay of s1s4KO PAX7-nGFP+ cells. Altogether, these results suggested specific deficiencies of s1s4KO PAX7+ cells to activate many genes that participated in establishing ECM and the niche required for their efficient homing and maturation during fetal development.

Neither MMP2, Mstn nor CXCR4 are required for PAX7+ cell homing during fetal myogenesis

Some studies suggest that PAX7+ cells need to cross the basal lamina to reach their niche (Alameddine et al., 1991; Hughes and Blau, 1990). Such a process may participate in efficient homing of PAX7+ cells in contact with primary myofibers (Fig. 2). We hypothesized that metalloproteinases might participate in this process and that a decreased *Mmp2* expression in s1s4KO PAX7+ cells could contribute to their homing deficiency. To test this hypothesis, we investigated PAX7+ cell location in E18.5 *Mmp2* KO back muscles and observed similar numbers of PAX7+ cells/ μm^2 and percentage of interstitial PAX7+ cells compared with the WT (Fig. S8A,B). Thus, absence of MMP2 did not affect PAX7+ cell homing during fetal myogenesis, suggesting that MMP2 was not involved in the homing of myogenic stem cells during fetal development.

In our study, the most upregulated gene in s1s4KO whole back muscles was encoding CXCL14 chemokine. This molecule can interact with CXCR4 and CXCR7 receptors, and this interaction could potentially counteract the CXCR4-SDF1 (also called CXCL12) pathway (Tanegashima et al., 2013a,b) that is involved in myogenic cell attraction (Vasyutina et al., 2005) and hematopoietic stem cell homing (Durand et al., 2018; Gao et al., 2018). Thus, we investigated PAX7+ cell homing in conditions where the CXCR4-SDF1 pathway was disrupted. We observed no deficiency in the homing process of PAX7+ cells in postnatal day (P) 0 animals lacking *Cxcr4* expression in the *Pax7* lineage (*Cxcr4^{lox/lox};Pax7^{CRE/+}*) (Fig. S8C,D). These results suggest that molecules signaling through CXCR4 were not required for PAX7+ cell homing, neither in PAX7+ cells nor in myofibers.

Last, we established that the number of PAX7+ cells under the basal lamina in back muscles of E18.5 *Mstn^{-/-}* fetuses (Matsakas et al., 2010) was not modified compared with controls (Fig. S8E,F), excluding the possibility that alteration of *Mstn* expression observed in s1s4KO fetuses was responsible for their homing deficiency; we

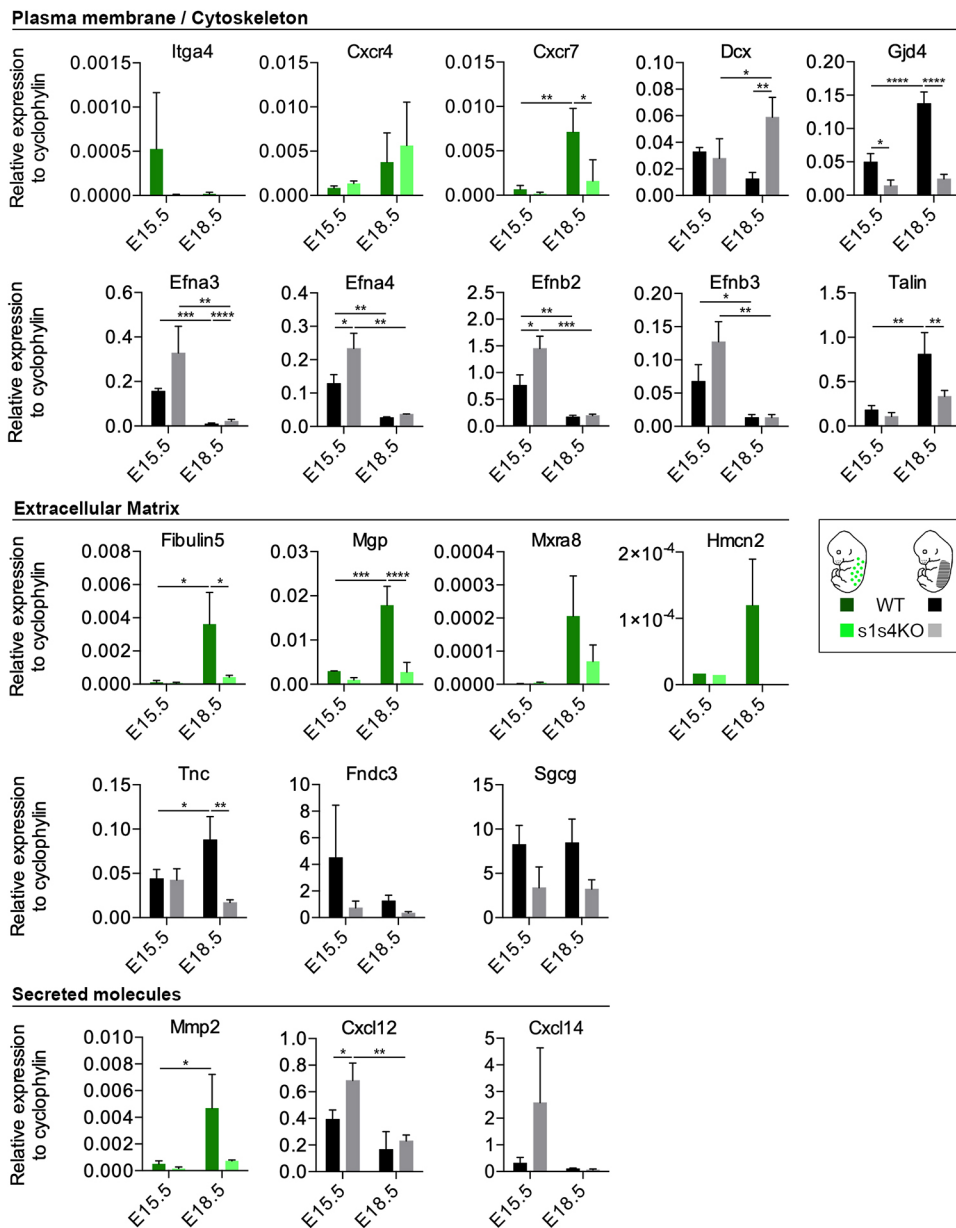


Fig. 5. Cell structure, ECM and secreted protein coding genes are mis-regulated in s1s4KO PAX7+ cells and whole back muscle tissue. qPCR validation of genes shown upregulated or downregulated in the Affymetrix analysis in PAX7+ cells (WT, dark green; s1s4KO, light green) or whole back muscles (WT, black; s1s4KO, gray) from E15.5 and E18.5 fetuses ($n=3$). * $P<0.05$, ** $P<0.01$, *** $P<0.001$, **** $P<0.0001$. Data are mean \pm s.d.

could not, however, exclude that alterations of TGF β /BMP signaling may participate in this phenotype.

Fetal s1s4KO PAX7+ cell transplantation into adult muscle yields hyperplastic atrophic denervated myofibers with a normal number of associated myogenic stem cells

To bypass s1s4KO lethality at birth, we transplanted E18.5 (one day before birth) s1s4Heterozygous (s1s4HZ) and s1s4KO Pax7-nGFP+ cells into adult tibialis anterior (TA) of immunodeficient mice after freeze injury. To reduce competition with endogenous PAX7+ cells, we used *Rag2*^{-/-} *γ C*^{-/-}*Pax7*^{DTR/+} mice and performed an intramuscular injection of Diphtheria toxin 5 h before injury and transplantation to eliminate endogenous PAX7+ cells (Sambasivan et al., 2011). s1s4KO cells were injected into one TA, and the contralateral muscle was injected with s1s4HZ cells as control. The *nls-lacZ* gene inserted at the *Six1* locus (Laclef et al., 2003a,b) allowed us to track myofibers formed from transplanted cells, as *Six1* is expressed in myonuclei of adult muscles (Laclef

et al., 2003a; Sakakibara et al., 2016). GFP expressed under the control of the *Pax7* promoter allowed us to track self-renewed PAX7-nGFP+ engrafted cells. Transplanted and injured TA were harvested 30 days post-injury (Fig. 6A,B). SIX1 immunostaining revealed that s1s4KO engrafted cells gave rise to s1s4KO myofibers with no endogenous host contribution; we only detected SIX1 protein in the host uninjured region of TA engrafted with s1s4KO cells and not in mutant myofibers (Fig. 6B). The approximate volume of the graft was similar between s1s4HZ and s1s4KO transplanted TA; however, the cross-sectional area (CSA) measurement indicating a fivefold decrease for mutant myofiber CSA showed that a higher number (hyperplasia) of small (hypotrophic) myofibers was formed compared with the control (Fig. 6C,D). Furthermore, although most newly formed control myofibers were fast (MY32+), with no expression of the fast embryonic (MYH3) myosin heavy chain and of the slow myosin heavy chain (MYH7), most s1s4KO myofibers were MY32+, MYH3+ and MYH7+ (Fig. S9A,B), in accordance with the known

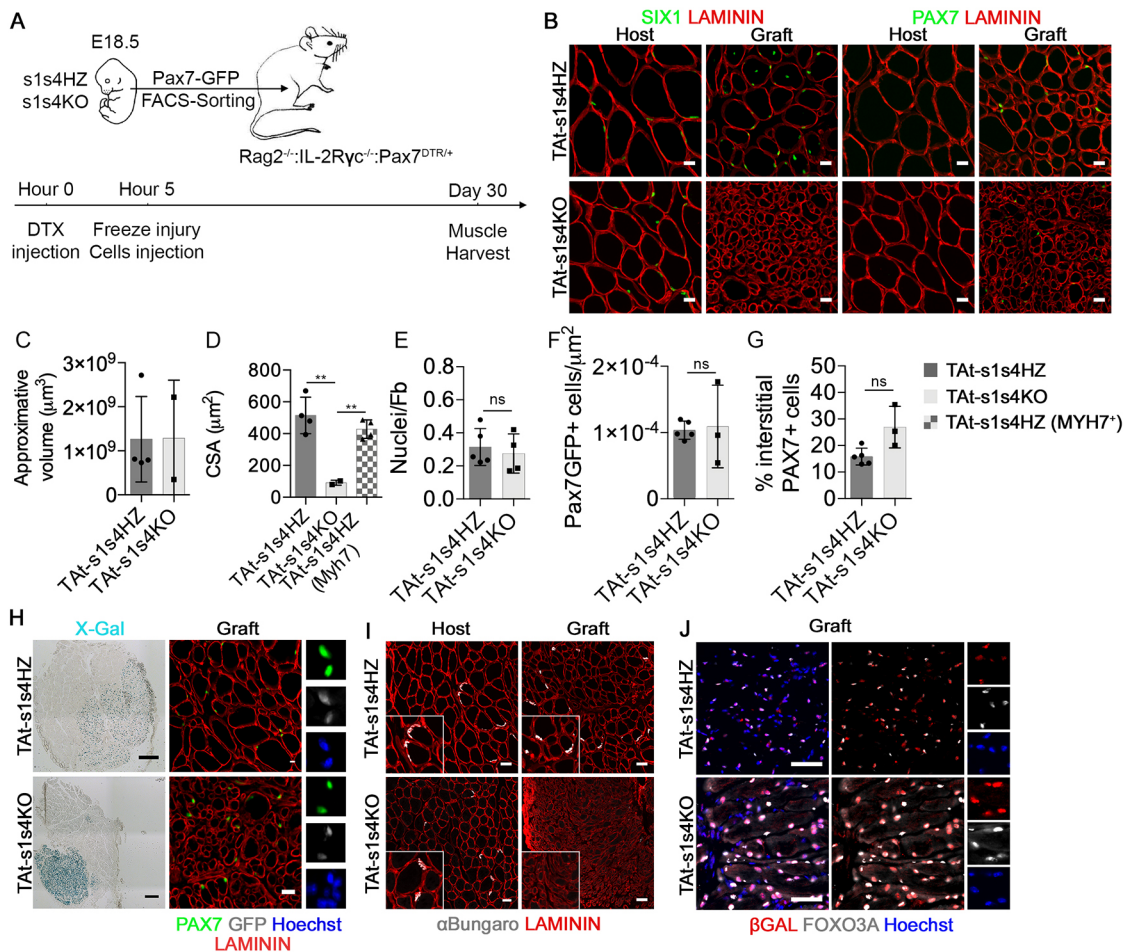


Fig. 6. Homing properties of fetal PAX7⁺ cells are different upon transplantation into adult muscles. (A) PAX7-GFP⁺ cells were FACS-sorted from E18.5 s1s4HZ or s1s4KO back muscles and transplanted into cryodamaged TA muscles of Rag2^{-/-};IL-2Rγc^{-/-};Pax7^{DTR/+} mice previously injected with Diphtheria toxin (DTX). Regenerated TA muscles were harvested 30 days after transplantation. (B) Immunostaining for SIX1 (green) or PAX7 (green) and laminin (red) in the host and graft regions of TA muscles transplanted with s1s4HZ or s1s4KO PAX7⁺ cells. (C-G) Quantification of the approximate graft volume (C), CSA (D), number of nuclei per fiber (E), number of PAX7GFP⁺ cells per μm² (F) and percentage of PAX7GFP⁺ interstitial cells (G) in the graft region of TA transplanted with s1s4HZ (*n*=4-5) or s1s4KO (*n*=3) PAX7GFP⁺ cells. (H-J) X-gal staining of Six1-*lacZ*⁺ cells shown on a whole transplanted TA section (left) and immunostaining for PAX7 (green), GFP (white) and laminin (red) in the graft region of TA muscles transplanted with s1s4HZ or s1s4KO PAX7⁺ cells (right). (I) Immunostaining for laminin (red) coupled with α-bungarotoxin reaction with acetylcholine receptors (white) in the host and graft regions of TA muscles transplanted with s1s4HZ or s1s4KO PAX7⁺ cells. (J) Immunostaining for β-gal (red) and FOXO3A (white) in the graft region of TA muscles transplanted with s1s4HZ or s1s4KO PAX7⁺ cells. In all panels nuclei are stained with Hoechst (blue). ***P*<0.01. Data are mean±s.d. Scale bars: 20 μm in B; 300 μm in H (X-gal staining); 20 μm in H (Graft); 50 μm in I, J.

role of these homeoproteins in the genesis and maintenance of the fast muscle phenotype (Grifone et al., 2004; Sakakibara et al., 2016). As slow myofibers usually have a smaller diameter, we validated that the CSA difference between s1s4HZ and s1s4KO myofibers was not due to their fiber-type (Fig. 6D). Because myofiber volume is related to myonuclear content, we assessed myonuclei number and found a small decrease in mutant myofibers (recapitulating the *in vitro* phenotype), indicating that impaired fusion could only partially account for the reduced CSA of mutant fibers (Fig. 6E). Therefore, fetal s1s4KO PAX7⁺GFP cells were able to proliferate and differentiate in the bed of the adult TA, and to give rise to numerous myofibers.

The number of self-renewed PAX7-nGFP⁺ cells was slightly reduced in KO-engrafted TA, but this was not statistically significant (Fig. 6F). There was a tendency towards an increased number of interstitial Pax7-nGFP⁺ cells compared with s1s4HZ PAX7-nGFP⁺ cells (Fig. 6B,G,H) in line with the observations made in E18.5 fetuses. Thus, although many genes coding for ECM were downregulated,

mutant PAX7⁺ cells were able to proliferate, to maintain myogenic identity, and to give rise to both myofibers and PAX7⁺ cells.

To determine whether the atrophic phenotype of newly formed s1s4KO myofibers was only due to the intrinsic absence of *Six1* and *Six4* expression or was also the consequence of innervation defects, as already observed in E18.5 s1s4KO fetuses (Richard et al., 2011), we assessed the presence of neuromuscular junctions (NMJ) on newly formed myofibers. We observed α-bungarotoxin accumulation in s1s4HZ engrafted TA (host and graft regions); however, we did not observe α-bungarotoxin accumulation in the grafted region of s1s4KO, even though the host region showed α-bungarotoxin accumulation (Fig. 6I). Thus, the NMJ did not form in the mutant graft and mutant myofibers were unable to attract WT motoneurons.

In contrast to the absence of reinnervation, CD31 (Pecam1) labeling showed that mutant grafts were efficiently revascularized in the graft of s1s4KO, suggesting that vascularization defects were not involved in the observed phenotype (Fig. S9C). As myofiber atrophy is orchestrated by FoxO nuclear accumulation, we examined

FoxO3A (FoxO3) expression and observed a more robust accumulation of FoxO3A in s1s4KO myonuclei compared with the s1s4HZ graft, suggesting an activation of the atrophy pathway in mutant regenerated myofibers (Fig. 6J).

DISCUSSION

In this study, we investigated the roles of the homeogenes *Six1* and *Six4* in muscle stem cells during fetal myogenesis. We showed that the homing process of PAX7+ cells is deficient in s1s4KO fetuses and that this phenotype correlates with the misregulation of many genes normally expressed in fetal PAX7+ cells and associated myofibers, leading to a distinct composition of the ECM in the absence of *Six1* and *Six4*. Transplantation of fetal mutant cells in adult injured TA muscle showed that generated myofibers were atrophic.

PAX7+ cell homing during fetal myogenesis is compromised in s1s4 mutant

An important aspect of stem cells is their microenvironment that controls their stemness properties (O'Brien and Bilder, 2013). Several cell types in the environment of adult PAX7+ myogenic stem cells modulate their behavior (Wosczyzna and Rando, 2018). Adult SCs establish contacts with the myofiber, for instance through M-cadherin (Cdh15) and Notch/Delta interactions, and they interact with the basal lamina that surrounds each myofiber. This matrix is composed of numerous proteins, among them laminins, with which they can interact via integrins (Montarras et al., 2013). When these contacts are established during development of the muscle system is unclear. PAX7+ cell homing occurs during fetal myogenesis, between E14.5-E18.5 in the mouse (Bröhl et al., 2012; Kassari-Duchossoy et al., 2005; Relaix et al., 2005). At E18.5 most PAX7+ cells are in close contact with myofibers in an SC position that allows them to further divide and participate in myofiber growth by nuclear accretion into myofibers. We observed that the homing evolved gradually during fetal myogenesis and started after E14.5. At this time, all PAX7+ cells are located in the interstitial space of growing muscle masses. At E16.5, confocal images identified PAX7+ cells in between basal lamina layers. Those cells could be crossing the basal lamina to enter their niche and establish contacts with primary myofibers, as suggested by previous publications (Hughes and Blau, 1990; Kowalski et al., 2017; Lafreniere et al., 2006; Webster et al., 2016). However, we cannot exclude the possibility that the matrix around primary myofibers is not continuous, allowing PAX7+ cells to contact primary myofibers without crossing a basal lamina (Bröhl et al., 2012; Kassari-Duchossoy et al., 2005; Relaix et al., 2005). We observed a decreased expression of MMP2 (Kherif et al., 1999), a metalloproteinase known to remodel the ECM that may impair migration of mutant cells through the ECM and participate in the homing deficiency. Analysis of E18.5 MMP2 mutants (Oh et al., 2004) revealed no homing deficiency, indicating that this protein has no major role on its own during the homing process of PAX7+ cells in the mouse fetus.

Efficient hematopoietic stem cells homing requires the CXCL12-Sdf-1/CXCR4 axis (reviewed by Pinho and Frenette, 2019). It is known that this Sdf-1/CXCR4 axis is an important chemoattractant of somitic myogenic progenitors in the embryonic limb buds (Vasyutina et al., 2005), but its involvement in the homing of PAX7+ cells has not yet been evaluated. We show here that, in the absence of *Cxcr4*, the homing of PAX7+ myogenic stem cells is not impaired, excluding a major role of this signaling pathway in myogenic stem cell homing. This hypothesis was strengthened by the strong overexpression of *Cxcl14* in s1s4KO cells that has been identified as an Sdf-1/CXCR4 competitor in some cases

(Tanegashima et al., 2013a,b). The absence of homing defects in *Cxcr4* KO muscles does not exclude an action of CXCL14 chemokine in the homing process through a different receptor.

SIX1 and SIX4 control the expression of many genes during fetal development

In *RBPJ^{lox/lox};Pax3^{CRE/+};MyoD^{-/-}* mutant, PAX3+ cells are impaired in their homing process, and NOTCH signaling is required for this process through direct myofiber-PAX3+ cells interaction and through expression of basal lamina components and adhesion molecules (Bröhl et al., 2012). However, we did not observe misregulation of NOTCH target genes in transcriptomic data. Among the genes downregulated in s1s4 mutants that may participate in the establishment of the ECM required for efficient PAX7+ cells homing are *Hmgn2*, *Mgp*, *Fbln5*, *Fnl1* and *Tnc*. HMCN2 (Feitosa et al., 2012; Jayadev and Sherwood, 2017) is a protein of the basement membrane and was identified as downregulated in NOTCH/MyoD mutant PAX7+ cells (Bröhl et al., 2012); its function in myogenic cells is not known. MGP is produced by both PAX7+ cells and the muscle at E15.5 and E18.5. This ECM protein is known to interfere with the interaction between MSTN and its ACVRIIB receptor (Ahmad et al., 2017) in the muscle lineage, and to antagonize BMP2 leading to reduced calcification in cartilage (Zebboudj et al., 2002). Fbln5, an integrin-binding protein (Yanagisawa et al., 2009), is known to modulate angiopoietin/Tie2 signaling in endothelial cells (Chan et al., 2016), a signaling pathway that triggers myogenic stem cell self-renewal (Abou-Khalil et al., 2009). *Fbln1* and *Fbln5* are expressed in PAX7+ cells: *Fbln5* is upregulated between E15.5-E18.5 in WT PAX7+ cells and may participate in assembling the basal lamina that is forming at that stage. We also show that several collagen genes, among them *Col6a6* and *Tnc*, are more expressed by WT PAX7+ cells and by the whole muscle during formation of the ECM that builds the PAX7+ cell niche between E15.5-E18.5. The role of these proteins in muscle ECM formation has previously been described (Baghdadi et al., 2018; Tierney and Sacco, 2016; Urciuolo et al., 2013) and their downregulation in mutant embryos may participate to the homing deficiency observed.

Homing deficiency of s1s4 mutant myogenic cells is not manifested after transplantation

We found that the percentage of PAX7+ cells located in the interstitial space of s1s4KO grafts was only slightly increased compared with the controls, suggesting that mutant cells have no major homing deficiency once they are transplanted in adult muscle. Several mechanisms might explain this result. First, PAX7+ cells transplanted into damaged muscle become directly located under the basal lamina. Indeed, intravital studies performed during muscle regeneration showed remaining ECM structures around damaged myofibers, called ghost fibers (Webster et al., 2016). If transplanted PAX7+ cells are injected directly inside ghost fibers, they might form a new myofiber within these basal lamina structures and this does not need to home extensively to contribute to muscle regeneration. Second, all cell types in s1s4KO fetuses lack *Six1* and *Six4* expression, whereas only PAX7+ cells and regenerated myofibers were mutant in the transplantation model. As other cell types, such as muscle resident fibroblasts, endothelial cells or motoneurons, may participate in the homing process during fetal development, we cannot exclude their contribution in the observed homing phenotype, especially as fibroblasts are known to produce collagens required for ECM assembly. Neither fetal nor transplanted muscles are innervated, and most PAX7+ cells are under the basal

lamina after transplantation, suggesting that the absence of innervation does not prevent PAX7⁺ cell homing, i.e. that genes coding for ECM produced by the myofibers are activated in non-innervated myofibers. Although the contribution of endogenous fibroblasts, fibroadipogenic progenitors, endothelial and inflammatory cells has been well documented in adult muscle regeneration (Wosczyzna and Rando, 2018), their potential contribution in the homing of fetal PAX7⁺ cells during development remains to be precisely evaluated. Third, the homing deficiency observed in mutant fetal muscles may arise from a delay due to decreased ECM formation. In contrast, in spite of this delay, grafting of mutant PAX7⁺ cells allowed ECM reconstitution 1 month after their transplantation. Finally, the homing process described during adult muscle regeneration after cardiotoxin/BaCl₂/freeze injury may be distinct to the homing process of myogenic stem cells that takes place during development. For example, inflammation might participate in homing in the adult but not during development (Webster et al., 2016; Wosczyzna and Rando, 2018).

Atrophy of s1s4 mutant myofibers

SC homing takes place when the muscle fiber number is reached before birth (Ontell and Kozeka, 1984; White et al., 2010). It is tempting to speculate that muscle growth during fetal development, which is associated with an increased number of myofibers, is favored when SCs are located outside the basal lamina, and that their sequestration must be tightly controlled to ensure a certain number of secondary myofibers within each muscle mass. Then, SCs become tightly associated with myofibers, where they continue to proliferate and participate in postnatal muscle hypertrophy by accretion of new nuclei in existing myofibers, before entering quiescence at around P21 (Kim et al., 2016; White et al., 2010).

Among the genes that we characterized in our transcriptomic analysis, none are directly linked with muscle atrophy. We also did not observe any atrophy in E18.5 s1s4KO back myofibers. s1s4 mutant epaxial muscle masses are characterized by hypoplasia that is observed from E14.5 at the end of primary myogenesis. Although E18.5 WT and mutant myofiber CSA were comparable, we observed that transplantation of E18.5 PAX7⁺ cells give rise to atrophic fibers with reduced CSA. *Ex vivo*, a major fusion deficit characterized mutant cells, leading to small myotubes with a low number of myonuclei. Nevertheless, following engraftment, mutant PAX7⁺ cells in adult injured TA muscle led to efficient regeneration characterized by a high number of regenerated myofibers with smaller diameter. Each of these mutant regenerated myofibers had a slightly reduced number of myonuclei compared with their heterozygote counterpart. The hypotrophy and hyperplastic muscle mass might be caused by cell intrinsic mechanisms or may involve the WT (host) environment. Indeed, we observed that mutant myofibers are not innervated. Although denervation is known to induce muscle atrophy, it is not known to induce muscle hyperplasia (Ashby et al., 1993). Contrary to s1s4HZ myofibers, mutant myofibers are not innervated, a phenotype reminiscent of the one observed in s1s4 mutant fetuses, for which we have already shown innervation defects (Richard et al., 2011). As in the transplantation experiments (this study) motoneurons arise from the host, we can suspect that mutant myofibers are unable to attract efficiently WT motoneurons, or that they produce too many repulsive molecules, precluding NMJ formation. Ephrins are involved in the repulsion of specific motoneurons (Stark et al., 2015), and may participate in both the denervation defects and PAX7⁺ homing delay observed in mutant embryos, as ephrin signaling leads to PAX7⁺ myogenic stem cell repulsion (Stark et al., 2011). Accordingly, ephrins A3, A4

and B3 and ephrin receptors A1, A3, A4 and A6 are upregulated 1.4- to 2-fold in mutant E15.5 muscle masses.

Muscle atrophy observed in the graft of s1s4KO myofibers may be the consequence of intrinsic mutant myofiber properties or due to innervation defects. We observed a robust FoxO3A nuclear accumulation in mutant myofibers present in the grafted TA. FoxO3A is a known effector of muscle atrophy induced by denervation and by a reduction of Akt activity (Bertaglia et al., 2012; Ratti et al., 2015); its accumulation in mutant myofibers may participate in their atrophic phenotype. A deficient Six4-Baf60c-Akt pathway may contribute to this increased FoxO3A activity (Meng et al., 2013).

Hyperplasia of s1s4 mutant muscles

Considering muscle hyperplasia, acquisition of a stereotyped number of fibers in each individualized muscle mass during development is a poorly understood mechanism. We suggest here that the equilibrium between PAX7⁺ cells directly contacting myofibers, which should allow efficient fusion with these myofibers, and interstitial PAX7⁺ cells, which should allow the generation of new myofibers, controls the correct number of myofibers. Muscle hyperplasia has been observed in a few mouse models such as in *Mstn*^{-/-} (Matsakas et al., 2010), in *Smad4*^{-/-} (Sartori et al., 2013) and in *Grb10* mutants (Mokbel et al., 2014), suggesting that the BMP and IGF1 pathways participate in the control of muscle mass not only by the control of hypertrophy, but also by the control of myofiber number. Whether the BMP/TGFβ pathways, known to be under the control of *Six1* in several cancer cells (Micalizzi et al., 2009; Nishimura et al., 2017; Patrick et al., 2013), are misregulated in s1s4KO myogenic cells remains to be firmly established. A link between SIX proteins and BMP signaling has been identified in zebrafish PAX7⁺ cells where the level of pSMAD1/5/8 and proliferation of PAX7⁺ cells are decreased in *Six1* mutants (Nord et al., 2013). We observed that many genes of this pathway are downregulated in s1s4 mutant PAX7⁺ cells or whole back dorsal muscle, including *Mstn*, *Tgfb3*, *Lthp1*, *Chrdl2*, *Bmper*, *Bmp4* and *Bmp7*, and the involvement of these genes in homing of myogenic stem cells remains to be established. Nevertheless, we show here that E18.5 *Mstn* mutants present a correct homing of PAX7⁺ cells in epaxial muscles, although many collagens are downregulated in *Mstn* mutant muscles (Welle et al., 2009), excluding the possibility that downregulation of this gene is responsible alone for the homing deficiency observed in s1s4KO fetuses.

In summary, we characterized the dynamic expression of genes in both PAX7⁺ myogenic stem cells and their associated daughter cells in myofibers during fetal development, with the aim of identifying molecules that participate in the crosstalk between PAX7⁺ cells and their progeny, and potential feedback loops required for efficient homing of PAX7⁺ cells in contact with their myofibers. The identification of several candidate genes that may be involved in this crucial process provides important insights into how muscle homeostasis is regulated.

MATERIALS AND METHODS

Mice and animal care

Animal experimentation was carried out in strict accordance with the European convention STE 123 and the French national charter on the Ethics of Animal Experimentation. Protocols were approved by the Ethical Committee of Animal Experiments of the Institut Cochin, CNRS UMR 8104, INSERM U1016 and by the Ministère de l'éducation nationale, de l'enseignement et de la recherche, APAFIS#15699-2018021516569195.

Six1^{-/-} and *Six1*^{-/-}*Six4*^{-/-} mutants, and their littermate control fetuses, were obtained by crossing *Six1*^{-/+} (Laclef et al., 2003a,b), *Six1*^{-/+}*Six4*^{-/+} (Grifone et al., 2005) 2- to 4-month-old mice respectively; they were backcrossed on the C57BL/6N background. *Six1*^{-/+}*Six4*^{-/+} mice were crossed with *Six5*^{-/-} mice (Klesert et al., 2000) to generate *Six1*^{-/-}*Six4*^{-/-}*Six5*^{-/-} and littermate control fetuses. *Six1*^{-/-}*Six4*^{-/-}*Tg:Pax7-nGFP/Pax7-nGFP* and *Six1*^{-/-}*Six4*^{-/-}*Six5*^{-/-}*Tg:Pax7-nGFP/Pax7-nGFP* mutants and their littermate control fetuses were obtained by crossing *Six1*^{-/+}*Six4*^{-/+}*Tg:Pax7-nGFP/Pax7-nGFP* and *Six1*^{-/+}*Six4*^{-/+}*Six5*^{-/+}*Tg:Pax7-nGFP/Pax7-nGFP* 2- to 4-month-old mice respectively; they were backcrossed on a C57BL/6N and DBA mixed background (Sambasivan et al., 2009). *Mmp2*^{-/-} and littermate control fetuses were kindly given by Dr T. Nakashiba (Riken BioResource Research Center, Tsukuba, Ibaraki, Japan) with the agreement of Dr S. Itohara (Itoh et al., 1997). *Cxcr4*^{lox/lox}*Pax7*^{CRE/+} fetuses and their littermate control were obtained on a C57BL/6N background. Transplantation experiments were performed on 2- to 4-month-old *Rag2*^{-/-}*γc*^{-/-} or *Rag2*^{-/-}*γc*^{-/-}*Pax7*^{DTR/+} mice (Colucci et al., 1999; Sambasivan et al., 2011). When needed, E18.5 pregnant females received 250 μl of a 10 mg/ml BrdU solution by intraperitoneal (IP) injection and were sacrificed 2 h after the pulse for fetus harvesting.

Fetus preparation

Fetuses were staged, taking the appearance of the vaginal plug as E0.5, harvested 14.5, 16.5 and 18.5 days post-fertilization, decapitated and their skin was removed (except for E14.5 fetuses). They were fixed in 4% paraformaldehyde (PFA) for 15 min (E14.5) or 30 min (E16.5 and E18.5) at room temperature and kept in 15% sucrose-PBS at 4°C overnight. Then they were embedded into OCT and snap frozen in isopentane (-30°C), cooled in liquid nitrogen and kept at -80°C until used. Transversal trunk 10 μm cryostat slices at the heart level were put on SuperFrost Plus glass slides (Thermo Fisher Scientific) and kept at -80°C until use.

Immunohistochemistry

Fetus sections were rehydrated in PBS before antigene retrieval treatment in a pH 6 citrate buffer solution at 95°C for 15 min plus 20 min cooling. They were permeabilized in 0.5% Triton X-100 for 30 min and blocked with 0.5% Triton X-100 and 5% horse serum for 3 h at room temperature. Primary and secondary antibodies were diluted in the blocking solution and incubated on the sections at 4°C overnight and 1 h at room temperature, respectively. Transplanted TA sections were rehydrated in PBS, permeabilized in 0.5% Triton X-100, blocked in 1.5% bovine serum albumin, 15% goat serum and 0.5% Triton X-100 and antibodies were diluted in the blocking solution. CD31 immunostainings required a special protocol: sections were permeabilized with cold -20°C acetone for 10 min and air dried for 10 min, then blocked and incubated with antibodies as described before. SIX1 immunostaining required an amplification step using a biotinylated secondary antibody. Sections were then incubated with streptavidin peroxidase-coupled for 30 min and revealed with 488 nm tyramide for 10 min (Thermo Fisher Scientific, Alexa Fluor™ 488 Signal-Amplification Kit, A11054). Immuno-stained sections were mounted under a coverslip with Dako fluorescent mounting medium before imaging. Images were taken on an Olympus BX63 upright fluorescent microscope, or on a Yokogawa CSU X1 spinning disk coupled with a DMI6000B Leica inverted microscope and acquisitions were made with an ORCA-Flash4.0 LT Hamamatsu camera or a CoolSnapHQ2 camera (Photometrics), respectively, using Metamorph 7 software. Primary myoblasts were fixed in 4% PFA for 10 min and blocked in 0.5% Triton X-100 and 5% horse serum for 30 min at room temperature. Primary and secondary antibodies were diluted in the blocking solution and incubated on the cells for 1 h at room temperature. Cells were mounted under a coverslip in Dako fluorescent mounting medium. Pictures were taken on a DMI6000 Leica inverted microscope and acquisitions were made with a Coolsnap HQ2 with Metamorph 7 software. See Table S13 for antibody references.

FACS isolation

Flow cytometry analyses were performed at the Cochin Flow Cytometry Facility. Mononucleated Pax7-nGFP⁺ cells were isolated from the back musculature of E14.5 and E18.5 fetuses. After removal of the skin,

fetuses were eviscerated, hind and forelimbs were removed as well as pelvis, ventral part of the rib cage, spinal cord and brown adipose tissue of the back. Remaining tissues were cut into small pieces with scissors, digested three times for 15 min at 37°C in a 1% trypsin 1% collagenase I DMEM-F12 solution. Digested tissues were filtered on 70 μm cell strainers and cells were centrifuged for 30 min at 1800 rpm (580 g). Pelleted cells were filtered on 30 μm cell strainers and kept in polypropylene tubes on ice until FACS. GFP⁺ cells were sorted using a BD FACSAria III cell sorter thanks to the BD FACSDIVA Software, collected into fetal calf serum, centrifuged at 2000 rpm (720 g) for 10 min and washed twice in PBS.

Microarray analysis

Microarray analyses were performed at the Cochin Genomic Facility on RNA extracted from E14.5 and E18.5 FACS-sorted Pax7-nGFP⁺ cells or whole back muscles. After validation of RNA quality with the Bioanalyzer 2100 (using Agilent RNA6000 nano chip kit), 50 ng (E18.5 whole back muscles), 2 ng (E15.5 FACS-sorted cells and whole back muscles) or 0.21 ng (E18.5 FACS-sorted cells) of total RNA were reverse-transcribed following the Ovation PicoSL or PicoV2 WTA System (Nugen). Briefly, the resulting double-stranded cDNA was used for amplification based on single primer isothermal amplification (SPIA) technology. After purification according to Nugen protocol, 5 μg of single-stranded DNA was used for generation of Sens Target DNA using Ovation Exon Module kit (Nugen). Then, 2.5 μg of Sens Target DNA were fragmented and labeled with biotin using the Encore Biotin Module kit (Nugen). After control of fragmentation using the Bioanalyzer 2100, the cDNA was then hybridized to GeneChip® Mouse Gene 1.0 or 2.0 ST (Affymetrix) at 45°C for 17 h. After overnight hybridization, the chips were washed using the fluidic station FS450 following specific protocols (Affymetrix) and scanned using the GCS3000 7G. The scanned images were then analyzed with Expression Console software (Affymetrix) to obtain raw data (cel files) and metrics for quality controls. Analysis of some of these metrics and the study of the distribution of raw data showed no outliers. Robust multiarray average (RMA) normalization was performed using R and normalized data were subjected to statistical tests. Data were analyzed using the ingenuity pathway analysis (IPA) software and the GSEA application.

RNA extraction and amplification

RNA extraction from Pax7-nGFP⁺ FACS-sorted cells was performed using the Qiagen RNeasy microkit directly after isolation. RNA quality was then validated with a Bioanalyzer 2100 and cDNA synthesis and amplification were performed based on SPIA technology mentioned above. RNA extraction from primary myoblasts or myotubes and from E14.5 and E18.5 whole back muscles was performed using the TRIzol kit (Thermo Fisher Scientific) following the manufacturer's protocols. Whole back muscles required a tissue lysis step in Trizol solution. RNAs were treated with DNase I (Turbo DNA-free, Invitrogen) and were reverse-transcribed using the Superscript III kit (Invitrogen) according to the manufacturer's instructions. Reverse transcription was performed with 50 ng (whole back muscles), 2 ng (E15.5 FACS-sorted Pax7-nGFP⁺ cells) or 0.2 ng (E18.5 FACS-sorted Pax7-nGFP⁺ cells) of total RNA. Quantitative real time PCRs (Light Cycler 480, Roche) were performed using Light Cycler 480 SYBR Green I Master Kit (Roche) according to the manufacturer's protocols. cDNA was amplified using 40 cycles of 95°C for 15 s, 60°C for 15 s and 72°C for 15 s. Gene expression levels were normalized to the expression level of the housekeeping gene cyclophilin (*Ppia*). Oligonucleotide sequences used in this study are listed in Table S14.

Transplantation

Rag2^{-/-}*γc*^{-/-} and *Rag2*^{-/-}*γc*^{-/-}*Pax7*^{DTR/+} immunodeficient mice, 2-4 months old, were used as recipients for FACS-sorted fetal Pax7-nGFP⁺ cell transplantation (Colucci et al., 1999; Sambasivan et al., 2011). After FACS isolation, myoblasts were centrifuged at 2000 rpm (720 g) for 10 min and the pellet was resuspended in sterile 1× PBS at 1000 cells/μl. Then, mice were anesthetized with an IP injection of 80 mg/kg ketamine hydrochloride and 10 mg/kg xylazine (Sigma-Aldrich, X1126) as described previously (Silva-Barbosa et al., 2005). TA muscles were subjected to three

consecutive cycles of freeze/thawing by applying a liquid nitrogen-cooled metallic rod on the muscle surface, preliminarily exposed by opening the skin. Both TA muscles were injected with 15,000 FACS-sorted cells resuspended in 15 μ l 1 \times PBS, one TA with *Six1*^{-/-}*Six4*^{-/-} cells and the contralateral with *Six1*^{+/+}*Six4*^{+/+} cells. Animals were sutured after injection. Analgesia was induced by IP injection with Buprenorphine (Axience, 0.03 mg/kg) at the end of the surgery. TA muscles were harvested 30 days post-transplantation. For the transplantation in *Rag2*^{-/-} γ C^{-/-}*Pax7*^{DTR/+}, Diphtheria toxin from *Corynebacterium diphtheriae* (Sigma Aldrich, D0564) was used for intra-muscular injection 5 h before cell transplantation at the concentration of 1.5 ng/g of total body mass (weight).

Adult muscle tissue preparation

Harvested TA muscles were directly fixed in 2% PFA, 0.2% Triton X-100 for 2 h at 4°C to preserve GFP reactivity. They were then incubated in 15% sucrose at 4°C overnight, embedded into OCT and snap frozen in isopentane (-30°C), cooled in liquid nitrogen and kept at -80°C until used. Transplanted TA were entirely cryosectioned into 10 μ m slices to find the grafted area.

X-gal staining

One section every 400 μ m of each transplanted TA was kept for 5-bromo-4-chloro-3-indolyl- β -D-galactopyranoside (X-gal) staining to find the grafted area owing to the *Six1-lacZ* reporter present in transplanted cells. Sections were stained with X-gal staining solution (1 mg/ml X-gal, 5 mM K₃Fe(CN)₆, 5 mM K₄Fe(CN)₆ and 2 mM MgCl₂ in 1 \times PBS) for 3 h at 37°C. Stained sections were mounted under a coverslip in glycerol gelatin. Images were taken with an Olympus BX63 upright microscope, using the Olympus DP73 high-performance Peltier cooled digital color camera.

Primary myoblast culture

After FACS isolation, cells were seeded on 1% Matrigel in PM containing 1:1 DMEM/F12, 20% fetal calf serum, 1 \times Ultrosor™ G and 1 \times antibiotic-antimycotic (anti-anti). At confluence, cells were trypsinized, centrifuged (260 g) and re-seeded at 1/3 decreased confluence for amplification. For experiments on proliferating myoblasts, cells were seeded on 1% Matrigel at 20,000 cells/cm² in PM and processed 12 h later. BrdU pulses were performed at 10 μ g/ml for 40 min at 37°C. For experiments on differentiated myotubes, myoblasts were seeded on 1% Matrigel at 40,000 cells/cm² in PM and 12 h later the PM was changed to DM composed of DMEM, 1 g/l glucose, 20% horse serum and 1 \times anti-anti. Cells were processed 3 or 6 days later. For proliferation assays, FACS-sorted cells were seeded on 1% Matrigel at 2500-5000 cells/cm² in PM. A 40 min BrdU pulse was performed 48 h later, before cell fixation.

Random cell migration assay

To measure random cell migration, 15,000 WT or *s1s4KO* myoblasts were seeded in a well of an Ibidi 8-well plate on Matrigel and left to attach overnight in PM. Time-lapse microscopy was used to image one picture every 6 min for 6 h. During imaging, the cells were left in PM and incubated at 37°C with 5% CO₂. Images were taken with a Zeiss Axio Observer.Z1 inverted microscope using the 10 \times objective; image acquisitions were made with an Orca Flash 4 OLT camera using Metamorph 7 software. Time-lapse analyses were performed using Imaris software.

Seahorse experiments

A Seahorse XF Cell Energy Phenotype Test Kit (103325-100, Agilent Technologies) was used to measure the oxygen consumption rate (OCR) and extracellular acidification rate (ECAR) on a Seahorse Bioscience XF96 Extracellular Flux Analyzer (Agilent Technologies). Pax7-GFP cells were seeded in XF96-well microplates (Agilent Technologies) at 2 \times 10⁴ cells/well 24 h before the Seahorse experiment. For each Seahorse experiment, the usual culture medium was changed to Seahorse medium plus 3.8 g/l glucose, 1 mM pyruvate and 200 μ M glutamine. Cells were then incubated at 37°C in the absence of CO₂ for 10 min. The plate was then introduced into the Seahorse Analyser for the real time analysis of OCR and ECAR in the basal state and after each addition of 1 μ M oligomycin, 1 μ M carbonyl

cyanide-p trifluoromethoxyphenylhydrazine (CCCP), 0.5 μ M CCCP and 2.5 μ M rotenone associated with 2.5 μ g/l antimycin. These different additions allowed testing the respiratory control (respiratory inhibition under complete inhibition of ATP production by oligomycin), the maximal respiratory capacity (maximal rate of respiration under uncoupling induced by the protonophore CCCP), and the non-respiratory oxygen consumption (residual OCR after complete respiration inhibition by rotenone, an inhibitor of complex I, and antimycin, an inhibitor of complex III). To normalize the OCR and ECAR results to cell number, the plate was briefly rinsed with PBS, incubated overnight at -20°C in 100 μ l 0.01% SDS per well, thawed and incubated for 1 h at room temperature with additional 100 μ l/well of Hoechst staining solution [4 μ g/ml Hoechst 33342, 1 M NaCl, 1 mM EDTA, 10 mM Tris HCl (pH 7.4)]. A plate fluorescence reader read the signal from the wells with cells, and from wells with serial dilutions of the commercially available lambda DNA/HindIII marker, allowing expression of the signal from the wells with cells as ng of DNA.

Statistical analysis

Two to five replicates were performed in the presented experiments. Data are mean \pm s.d. Results were assessed for statistical significance using a Mann-Whitney non-parametric significance test when comparing two groups, or a two-way regular Anova test when comparing more than two groups (Prism software). Significant differences were shown as follows: **P*<0.05, ***P*<0.01, ****P*<0.001, *****P*<0.0001.

Acknowledgements

We thank Dr S. Itohara and Dr T. Nakashiba for MMP2 KO fetuses. We thank Dr A. Lombès and F. Bouillaud for helpful advice with the Seahorse experiments, M. Andrieu and the CYBIO platform of I. Cochin for FACS experiments, and Dr E. Bloch-Gallego for helpful critical reading of the manuscript.

Competing interests

The authors declare no competing or financial interests.

Author contributions

Conceptualization: M.W., F.L.G., A.S., P.M.; Methodology: M.W., N.C., R.M., H.S., B.S.-P., V.M., F.L.G., P.M.; Software: M.W., B.S.-P.; Validation: M.W., N.C., R.M., P.M.; Formal analysis: M.W., N.C., R.M., A.S., P.M.; Investigation: M.W., N.C., R.M., H.S., E.N., J.D., A.S., P.M.; Resources: V.M., H.A., S. Tapscott, C.B., S. Tajbakhsh, P.M.; Data curation: M.W., P.M.; Writing - original draft: M.W., P.M.; Writing - review & editing: H.A., C.B., S. Tajbakhsh, A.S., P.M.; Supervision: A.S., P.M.; Project administration: P.M.; Funding acquisition: H.A., S. Tajbakhsh, P.M.

Funding

M.W. was supported by successive fellowships from the University de Paris, the Association Française contre les Myopathies (AFM), and the Agence Nationale de la Recherche (ANR) (ANR-16-CE14-0032-01). Financial support was provided by the AFM (16427 and 17406), the ANR (ANR-16-CE14-0002-01), the Institut National de la Santé et de la Recherche Médicale (INSERM) and the Centre National de la Recherche Scientifique (CNRS). S.T. acknowledges funding support from Institut Pasteur, ANR (Laboratoire d'Excellence Revive, Investissement d'Avenir; ANR-10-LABX-73).

Data availability

Microarray data have been deposited in Gene Expression Omnibus under accession number GSE159079.

Supplementary information

Supplementary information available online at <https://dev.biologists.org/lookup/doi/10.1242/dev.185975.supplemental>

References

- Abou-Khalil, R., Le Grand, F., Pallafacchina, G., Valable, S., Authier, F.-J., Rudnicki, M. A., Gherardi, R. K., Germain, S., Chretien, F., Sotiropoulos, A. et al. (2009). Autocrine and paracrine angiopoietin 1/Tie-2 signaling promotes muscle satellite cell self-renewal. *Cell Stem Cell* **5**, 298-309. doi:10.1016/j.stem.2009.06.001
- Ahmad, S., Jan, A. T., Baig, M. H., Lee, E. J. and Choi, I. (2017). Matrix gla protein: an extracellular matrix protein regulates myostatin expression in the muscle developmental program. *Life Sci.* **172**, 55-63. doi:10.1016/j.lfs.2016.12.011
- Alameddine, H. S., Hantai, D., Dehaupas, M. and Fardeau, M. (1991). Role of persisting basement membrane in the reorganization of myofibres originating from

- myogenic cell grafts in the rat. *Neuromuscul. Disord.* **1**, 143-152. doi:10.1016/0960-8966(91)90062-W
- Ashby, P. R., Pinçon-Raymond, M. and Harris, A. J. (1993). Regulation of myogenesis in paralyzed muscles in the mouse mutants peroneal muscular atrophy and muscular dysgenesis. *Dev. Biol.* **156**, 529-536. doi:10.1006/dbio.1993.1099
- Baghdadi, M. B., Castel, D., Machado, L., Fukada, S.-I., Birk, D. E., Relaix, F., Tajbakhsh, S. and Mourikis, P. (2018). Reciprocal signalling by Notch-Collagen V-CALCR retains muscle stem cells in their niche. *Nature* **557**, 714-718. doi:10.1038/s41586-018-0144-9
- Bentzinger, C. F., Wang, Y. X. and Rudnicki, M. A. (2012). Building muscle: molecular regulation of myogenesis. *Cold Spring Harb. Perspect. Biol.* **4**, a008342. doi:10.1101/cshperspect.a008342
- Bentzinger, C. F., Wang, Y. X., von Maltzahn, J., Soleimani, V. D., Yin, H. and Rudnicki, M. A. (2013). Fibronectin regulates Wnt7a signaling and satellite cell expansion. *Cell Stem Cell* **12**, 75-87. doi:10.1016/j.stem.2012.09.015
- Bertaglia, E., Coletto, L. and Sandri, M. (2012). Posttranslational modifications control FoxO3 activity during denervation. *Am. J. Physiol. Cell Physiol.* **302**, C587-C596. doi:10.1152/ajpcell.00142.2011
- Biressi, S., Molinaro, M. and Cossu, G. (2007). Cellular heterogeneity during vertebrate skeletal muscle development. *Dev. Biol.* **308**, 281-293. doi:10.1016/j.ydbio.2007.06.006
- Bjornson, C. R., Cheung, T. H., Liu, L., Tripathi, P. V., Steeper, K. M. and Rando, T. A. (2012). Notch signaling is necessary to maintain quiescence in adult muscle stem cells. *Stem Cells* **30**, 232-242. doi:10.1002/stem.773
- Borello, U., Berarducci, B., Murphy, P., Bajard, L., Buffa, V., Piccolo, S., Buckingham, M. and Cossu, G. (2006). The Wnt/beta-catenin pathway regulates Gli-mediated Myf5 expression during somitogenesis. *Development* **133**, 3723-3732. doi:10.1242/dev.02517
- Bröhl, D., Vasyutina, E., Czajkowski, M. T., Griger, J., Rassek, C., Rahn, H.-P., Purfürst, B., Wende, H. and Birchmeier, C. (2012). Colonization of the satellite cell niche by skeletal muscle progenitor cells depends on Notch signals. *Dev. Cell* **23**, 469-481. doi:10.1016/j.devcel.2012.07.014
- Buckingham, M. and Relaix, F. (2015). PAX3 and PAX7 as upstream regulators of myogenesis. *Semin. Cell Dev. Biol.* **44**, 115-125. doi:10.1016/j.semcdb.2015.09.017
- Buckingham, M. and Vincent, S. D. (2009). Distinct and dynamic myogenic populations in the vertebrate embryo. *Curr. Opin. Genet. Dev.* **19**, 444-453. doi:10.1016/j.gde.2009.08.001
- Chakroun, I., Yang, D., Girgis, J., Gunasekharan, A., Phenix, H., Kaern, M. and Blais, A. (2015). Genome-wide association between Six4, MyoD, and the histone demethylase Utx during myogenesis. *FASEB J.* **29**, 4738-4755. doi:10.1096/fj.15-277053
- Chan, W., Ismail, H., Mayaki, D., Sanchez, V., Tiedemann, K., Davis, E. C. and Hussain, S. N. (2016). Fibulin-5 regulates angiotensin-1/Tie-2 receptor signaling in endothelial cells. *PLoS ONE* **11**, e0156994. doi:10.1371/journal.pone.0156994
- Colucci, F., Soudais, C., Rosmaraki, E., Vanes, L., Tybulewicz, V. L. and Di Santo, J. P. (1999). Dissecting NK cell development using a novel alymphoid mouse model: investigating the role of the c-abl proto-oncogene in murine NK cell differentiation. *J. Immunol.* **162**, 2761-2765.
- Comai, G. and Tajbakhsh, S. (2014). Molecular and cellular regulation of skeletal myogenesis. *Curr. Top. Dev. Biol.* **110**, 1-73. doi:10.1016/B978-0-12-405943-6.00001-4
- Durand, C., Chabord, P. and Jaffredo, T. (2018). The crosstalk between hematopoietic stem cells and their niches. *Curr. Opin. Hematol.* **25**, 285-289. doi:10.1097/MOH.0000000000000438
- Duxson, M. J., Usson, Y. and Harris, A. J. (1989). The origin of secondary myotubes in mammalian skeletal muscles: ultrastructural studies. *Development* **107**, 743-750.
- Esteves de Lima, J., Bonnin, M. A., Birchmeier, C. and Duprez, D. (2016). Muscle contraction is required to maintain the pool of muscle progenitors via YAP and NOTCH during fetal myogenesis. *Elife* **5**, e15593. doi:10.7554/eLife.15593
- Evano, B. and Tajbakhsh, S. (2018). Skeletal muscle stem cells in comfort and stress. *NPJ Regen. Med.* **3**, 24. doi:10.1038/s41536-018-0062-3
- Feige, P., Brun, C. E., Ritso, M. and Rudnicki, M. A. (2018). Orienting muscle stem cells for regeneration in homeostasis, aging, and disease. *Cell Stem Cell* **23**, 653-664. doi:10.1016/j.stem.2018.10.006
- Feitosa, N. M., Zhang, J., Carney, T. J., Metzger, M., Korzh, V., Bloch, W. and Hammerschmidt, M. (2012). Hemicentin 2 and Fibulin 1 are required for epidermal-dermal junction formation and fin mesenchymal cell migration during zebrafish development. *Dev. Biol.* **369**, 235-248. doi:10.1016/j.ydbio.2012.06.023
- Fukada, S.-I., Akimoto, T. and Sotiropoulos, A. (2020). Role of damage and management in muscle hypertrophy: different behaviors of muscle stem cells in regeneration and hypertrophy. *Biochim. Biophys. Acta. Mol. Cell Res.* **1867**, 118742. doi:10.1016/j.bbmr.2020.118742
- Gao, X., Xu, C., Asada, N. and Frenette, P. S. (2018). The hematopoietic stem cell niche: from embryo to adult. *Development* **145**, dev139691. doi:10.1242/dev.139691
- Grifone, R., Laclef, C., Spitz, F., Lopez, S., Demignon, J., Guidotti, J.-E., Kawakami, K., Xu, P. X., Kelly, R., Petrof, B. J. et al. (2004). Six1 and Eya1 expression can reprogram adult muscle from the slow-twitch phenotype into the fast-twitch phenotype. *Mol. Cell. Biol.* **24**, 6253-6267. doi:10.1128/MCB.24.14.6253-6267.2004
- Grifone, R., Demignon, J., Houbron, C., Souil, E., Niro, C., Seller, M. J., Hamard, G. and Maire, P. (2005). Six1 and Six4 homeoproteins are required for Pax3 and Mrf expression during myogenesis in the mouse embryo. *Development* **132**, 2235-2249. doi:10.1242/dev.01773
- Gros, J., Manceau, M., Thomé, V. and Marcelle, C. (2005). A common somitic origin for embryonic muscle progenitors and satellite cells. *Nature* **435**, 954-958. doi:10.1038/nature03572
- Gros, J., Serralbo, O. and Marcelle, C. (2009). WNT11 acts as a directional cue to organize the elongation of early muscle fibres. *Nature* **457**, 589-593. doi:10.1038/nature07564
- Guerci, A., Lahoute, C., Hébrard, S., Collard, L., Graindorge, D., Favier, M., Cagnard, N., Batonnet-Pichon, S., Précigout, G., Garcia, L. et al. (2012). Srf-dependent paracrine signals produced by myofibers control satellite cell-mediated skeletal muscle hypertrophy. *Cell Metab.* **15**, 25-37. doi:10.1016/j.cmet.2011.12.001
- Hughes, S. M. and Blau, H. M. (1990). Migration of myoblasts across basal lamina during skeletal muscle development. *Nature* **345**, 350-353. doi:10.1038/345350a0
- Hutchesson, D. A., Zhao, J., Merrell, A., Haldar, M. and Kardon, G. (2009). Embryonic and fetal limb myogenic cells are derived from developmentally distinct progenitors and have different requirements for beta-catenin. *Genes Dev.* **23**, 997-1013. doi:10.1101/gad.1769009
- Itoh, T., Ikeda, T., Gomi, H., Nakao, S., Suzuki, T. and Itoharu, S. (1997). Unaltered secretion of beta-amyloid precursor protein in gelatinase A (matrix metalloproteinase 2)-deficient mice. *J. Biol. Chem.* **272**, 22389-22392. doi:10.1074/jbc.272.36.22389
- Jayadev, R. and Sherwood, D. R. (2017). Basement membranes. *Curr. Biol.* **27**, R207-R211. doi:10.1016/j.cub.2017.02.006
- Kassar-Duchossoy, L., Giaccone, E., Gayraud-Morel, B., Jory, A., Gomes, D. and Tajbakhsh, S. (2005). Pax3/Pax7 mark a novel population of primitive myogenic cells during development. *Genes Dev.* **19**, 1426-1431. doi:10.1101/gad.345505
- Kawakami, K., Ohto, H., Takizawa, T. and Saito, T. (1996). Identification and expression of six family genes in mouse retina. *FEBS Lett.* **393**, 259-263. doi:10.1016/0014-5793(96)00899-X
- Kelly, A. M. and Zacks, S. I. (1969). The histogenesis of rat intercostal muscle. *J. Cell Biol.* **42**, 135-153. doi:10.1083/jcb.42.1.135
- Kherif, S., Lafuma, C., Dehaupas, M., Lachkar, S., Fournier, J.-G., Verdière-Sahuqué, M., Fardeau, M. and Alameddine, H. S. (1999). Expression of matrix metalloproteinases 2 and 9 in regenerating skeletal muscle: a study in experimentally injured and mdx muscles. *Dev. Biol.* **205**, 158-170. doi:10.1006/dbio.1998.9107
- Kim, J.-H., Han, G.-C., Seo, J.-Y., Park, I., Park, W., Jeong, H.-W., Lee, S. H., Bae, S.-H., Seong, J., Yum, M.-K. et al. (2016). Sex hormones establish a reserve pool of adult muscle stem cells. *Nat. Cell Biol.* **18**, 930-940. doi:10.1038/ncb3401
- Klesert, T. R., Cho, D. H., Clark, J. I., Maylie, J., Adelman, J., Snider, L., Yuen, E. C., Soriano, P. and Tapscott, S. J. (2000). Mice deficient in Six5 develop cataracts: implications for myotonic dystrophy. *Nat. Genet.* **25**, 105-109. doi:10.1038/75490
- Kowalski, K., Kolodziejczyk, A., Sikorska, M., Placzkiewicz, J., Cichosz, P., Kowalewska, M., Stremińska, W., Jańczyk-Ilach, K., Kobłowska, M., Fogtman, A. et al. (2017). Stem cells migration during skeletal muscle regeneration - the role of Sdf-1/Cxcr4 and Sdf-1/Cxcr7 axis. *Cell Adh. Migr.* **11**, 384-398. doi:10.1080/19336918.2016.1227911
- Laclef, C., Hamard, G., Demignon, J., Souil, E., Houbron, C. and Maire, P. (2003a). Altered myogenesis in Six1-deficient mice. *Development* **130**, 2239-2252. doi:10.1242/dev.00440
- Laclef, C., Souil, E., Demignon, J. and Maire, P. (2003b). Thymus, kidney and craniofacial abnormalities in Six 1 deficient mice. *Mech. Dev.* **120**, 669-679. doi:10.1016/S0925-4773(03)00065-0
- Lafreniere, J. F., Mills, P., Bouchentouf, M. and Tremblay, J. P. (2006). Interleukin-4 improves the migration of human myogenic precursor cells in vitro and in vivo. *Exp. Cell Res.* **312**, 1127-1141. doi:10.1016/j.yexcr.2006.01.002
- Le Grand, F., Grifone, R., Mourikis, P., Houbron, C., Gigaud, C., Pujol, J., Maillet, M., Pagès, G., Rudnicki, M., Tajbakhsh, S. et al. (2012). Six1 regulates stem cell repair potential and self-renewal during skeletal muscle regeneration. *J. Cell Biol.* **198**, 815-832. doi:10.1083/jcb.201201050
- Lepper, C. and Fan, C.-M. (2010). Inducible lineage tracing of Pax7-descendant cells reveals embryonic origin of adult satellite cells. *Genesis* **48**, 424-436. doi:10.1002/dvg.20630
- Lepper, C., Partridge, T. A. and Fan, C.-M. (2011). An absolute requirement for Pax7-positive satellite cells in acute injury-induced skeletal muscle regeneration. *Development* **138**, 3639-3646. doi:10.1242/dev.067595
- Li, L., Liang, Y., Kang, L., Liu, Y., Gao, S., Chen, S., Li, Y., You, W., Dong, Q., Hong, T. et al. (2018). Transcriptional regulation of the warburg effect in cancer by SIX1. *Cancer Cell* **33**, 368-385.e367. doi:10.1016/j.ccell.2018.01.010
- Liu, Y., Chakroun, I., Yang, D., Horner, E., Liang, J., Aziz, A., Chu, A., De Repentigny, Y., Dilworth, F. J., Kothary, R. et al. (2013). Six1 regulates MyoD

- expression in adult muscle progenitor cells. *PLoS ONE* **8**, e67762. doi:10.1371/journal.pone.0067762
- Maire, P., Dos Santos, M., Madani, R., Sakakibara, I., Viaut, C. and Wurmser, M.** (2020). Myogenesis control by SIX transcriptional complexes. *Semin. Cell Dev. Biol.* **104**, 51-64. doi:10.1016/j.semdcb.2020.03.003
- Matsakas, A., Otto, A., Elashry, M. I., Brown, S. C. and Patel, K.** (2010). Altered primary and secondary myogenesis in the myostatin-null mouse. *Rejuvenation Res.* **13**, 717-727. doi:10.1089/rej.2010.1065
- Mauro, A.** (1961). Satellite cell of skeletal muscle fibers. *J. Biophys. Biochem. Cytol.* **9**, 493-495. doi:10.1083/jcb.9.2.493
- Meng, Z.-X., Li, S., Wang, L., Ko, H. J., Lee, Y., Jung, D. Y., Okutsu, M., Yan, Z., Kim, J. K. and Lin, J. D.** (2013). Baf60c drives glycolytic metabolism in the muscle and improves systemic glucose homeostasis through Deptor-mediated Akt activation. *Nat. Med.* **19**, 640-645. doi:10.1038/nm.3144
- Micalizzi, D. S., Christensen, K. L., Jedlicka, P., Coletta, R. D., Barón, A. E., Harell, J. C., Horwitz, K. B., Billheimer, D., Heichman, K. A., Welm, A. L. et al.** (2009). The Six1 homeoprotein induces human mammary carcinoma cells to undergo epithelial-mesenchymal transition and metastasis in mice through increasing TGF-beta signaling. *J. Clin. Invest.* **119**, 2678-2690. doi:10.1172/JCI37815
- Mokbel, N., Hoffman, N. J., Girgis, C. M., Small, L., Turner, N., Daly, R. J., Cooney, G. J. and Holt, L. J.** (2014). Grb10 deletion enhances muscle cell proliferation, differentiation and GLUT4 plasma membrane translocation. *J. Cell. Physiol.* **229**, 1753-1764. doi:10.1002/jcp.24628
- Montarras, D., L'Honore, A. and Buckingham, M.** (2013). Lying low but ready for action: the quiescent muscle satellite cell. *FEBS J.* **280**, 4036-4050. doi:10.1111/febs.12372
- Mourikis, P., Gopalakrishnan, S., Sambasivan, R. and Tajbakhsh, S.** (2012a). Cell-autonomous Notch activity maintains the temporal specification potential of skeletal muscle stem cells. *Development* **139**, 4536-4548. doi:10.1242/dev.084756
- Mourikis, P., Sambasivan, R., Castel, D., Rocheteau, P., Bizzarro, V. and Tajbakhsh, S.** (2012b). A critical requirement for notch signaling in maintenance of the quiescent skeletal muscle stem cell state. *Stem Cells* **30**, 243-252. doi:10.1002/stem.775
- Murphy, M. M., Lawson, J. A., Mathew, S. J., Hutcheson, D. A. and Kardon, G.** (2011). Satellite cells, connective tissue fibroblasts and their interactions are crucial for muscle regeneration. *Development* **138**, 3625-3637. doi:10.1242/dev.064162
- Nishimura, T., Tamaoki, M., Komatsuzaki, R., Oue, N., Taniguchi, H., Komatsu, M., Aoyagi, K., Minashi, K., Chiwaki, F., Shinohara, H. et al.** (2017). SIX1 maintains tumor basal cells via transforming growth factor-beta pathway and associates with poor prognosis in esophageal cancer. *Cancer Sci.* **108**, 216-225. doi:10.1111/cas.13135
- Nord, H., Nygard Skalmann, L. and von Hofsten, J.** (2013). Six1 regulates proliferation of Pax7-positive muscle progenitors in zebrafish. *J. Cell Sci.* **126**, 1868-1880. doi:10.1242/jcs.119917
- O'Brien, L. E. and Bilder, D.** (2013). Beyond the niche: tissue-level coordination of stem cell dynamics. *Annu. Rev. Cell Dev. Biol.* **29**, 107-136. doi:10.1146/annurev-cellbio-101512-122319
- Oh, J., Takahashi, R., Adachi, E., Kondo, S., Kuratomi, S., Noma, A., Alexander, D. B., Motoda, H., Okada, A., Seiki, M. et al.** (2004). Mutations in two matrix metalloproteinase genes, MMP-2 and MT1-MMP, are synthetic lethal in mice. *Oncogene* **23**, 5041-5048. doi:10.1038/sj.onc.1207688
- Oliver, G., Wehr, R., Jenkins, N. A., Copeland, N. G., Cheyette, B. N., Hartenstein, V., Zipursky, S. L. and Gruss, P.** (1995). Homeobox genes and connective tissue patterning. *Development* **121**, 693-705.
- Ontell, M. and Kozeka, K.** (1984). Organogenesis of the mouse extensor digitorum logus muscle: a quantitative study. *Am. J. Anat.* **171**, 149-161. doi:10.1002/aja.1001710203
- Ozaki, H., Watanabe, Y., Takahashi, K., Kitamura, K., Tanaka, A., Urase, K., Momoi, T., Sudo, K., Sakagami, J., Asano, M. et al.** (2001). Six4, a putative myogenic gene regulator, is not essential for mouse embryonal development. *Mol. Cell. Biol.* **21**, 3343-3350. doi:10.1128/MCB.21.10.3343-3350.2001
- Patrick, A. N., Cabrera, J. H., Smith, A. L., Chen, X. S., Ford, H. L. and Zhao, R.** (2013). Structure-function analyses of the human SIX1-EYA2 complex reveal insights into metastasis and BOR syndrome. *Nat. Struct. Mol. Biol.* **20**, 447-453. doi:10.1038/nsmb.2505
- Picard, C. A. and Marcelle, C.** (2013). Two distinct muscle progenitor populations coexist throughout amniote development. *Dev. Biol.* **373**, 141-148. doi:10.1016/j.ydbio.2012.10.018
- Pinho, S. and Frenette, P. S.** (2019). Haematopoietic stem cell activity and interactions with the niche. *Nat. Rev. Mol. Cell Biol.* **20**, 303-320. doi:10.1038/s41580-019-0103-9
- Ratti, F., Ramond, F., Moncollin, V., Simonet, T., Milan, G., Méjat, A., Thomas, J.-L., Streichenberger, N., Gilquin, B., Matthias, P. et al.** (2015). Histone deacetylase 6 is a FoxO transcription factor-dependent effector in skeletal muscle atrophy. *J. Biol. Chem.* **290**, 4215-4224. doi:10.1074/jbc.M114.600916
- Rayagiri, S. S., Ranaldi, D., Raven, A., Mohamad Azhar, N. I. F., Lefebvre, O., Zammit, P. S. and Borycki, A.-G.** (2018). Basal lamina remodeling at the skeletal muscle stem cell niche mediates stem cell self-renewal. *Nat. Commun.* **9**, 1075. doi:10.1038/s41467-018-03425-3
- Relaix, F., Rocancourt, D., Mansouri, A. and Buckingham, M.** (2005). A Pax3/Pax7-dependent population of skeletal muscle progenitor cells. *Nature* **435**, 948-953. doi:10.1038/nature03594
- Relaix, F., Demignon, J., Laclef, C., Pujol, J., Santolini, M., Niro, C., Lagha, M., Rocancourt, D., Buckingham, M. and Maire, P.** (2013). Six homeoproteins directly activate Myod expression in the gene regulatory networks that control early myogenesis. *PLoS Genet.* **9**, e1003425. doi:10.1371/journal.pgen.1003425
- Richard, A.-F., Demignon, J., Sakakibara, I., Pujol, J., Favier, M., Strohlic, L., Le Grand, F., Sgaroto, N., Guernec, A., Schmitt, A. et al.** (2011). Genesis of muscle fiber-type diversity during mouse embryogenesis relies on Six1 and Six4 gene expression. *Dev. Biol.* **359**, 303-320. doi:10.1016/j.ydbio.2011.08.010
- Rocheteau, P., Gayraud-Morel, B., Siegl-Cachedenier, I., Blasco, M. A. and Tajbakhsh, S.** (2012). A subpopulation of adult skeletal muscle stem cells retains all template DNA strands after cell division. *Cell* **148**, 112-125. doi:10.1016/j.cell.2011.11.049
- Rosen, G. D., Sanes, J. R., LaChance, R., Cunningham, J. M., Roman, J. and Dean, D. C.** (1992). Roles for the integrin VLA-4 and its counter receptor VCAM-1 in myogenesis. *Cell* **69**, 1107-1119. doi:10.1016/0092-8674(92)90633-N
- Rudolf, A., Schirwis, E., Giordani, L., Parisi, A., Lepper, C., Taketo, M. M. and Le Grand, F.** (2016). beta-catenin activation in muscle progenitor cells regulates tissue repair. *Cell Rep.* **15**, 1277-1290. doi:10.1016/j.celrep.2016.04.022
- Ryall, J. G.** (2013). Metabolic reprogramming as a novel regulator of skeletal muscle development and regeneration. *FEBS J.* **280**, 4004-4013. doi:10.1111/febs.12189
- Sakakibara, I., Wurmser, M., Dos Santos, M., Santolini, M., Ducommun, S., Davaze, R., Guernec, A., Sakamoto, K. and Maire, P.** (2016). Six1 homeoprotein drives myofiber type IIA specialization in soleus muscle. *Skelet Muscle* **6**, 30. doi:10.1186/s13395-016-0102-x
- Sambasivan, R., Gayraud-Morel, B., Dumas, G., Cimper, C., Paisant, S., Kelly, R. G. and Tajbakhsh, S.** (2009). Distinct regulatory cascades govern extraocular and pharyngeal arch muscle progenitor cell fates. *Dev. Cell* **16**, 810-821. doi:10.1016/j.devcel.2009.05.008
- Sambasivan, R., Yao, R., Kissenfennig, A., Van Wittenberghe, L., Paldi, A., Gayraud-Morel, B., Guenou, H., Malissen, B., Tajbakhsh, S. and Galy, A.** (2011). Pax7-expressing satellite cells are indispensable for adult skeletal muscle regeneration. *Development* **138**, 3647-3656. doi:10.1242/dev.067587
- Santolini, M., Sakakibara, I., Gauthier, M., Ribas-Aulinas, F., Takahashi, H., Sawasaki, T., Mouly, V., Concordet, J.-P., Defossez, P.-A., Hakim, V. et al.** (2016). MyoD reprogramming requires Six1 and Six4 homeoproteins: genome-wide cis-regulatory module analysis. *Nucleic Acids Res.* **44**, 8621-8640. doi:10.1093/nar/gkw512
- Sartori, R., Schirwis, E., Blaauw, B., Bortolanza, S., Zhao, J., Enzo, E., Stantzou, A., Mousel, E., Toniolo, L., Ferry, A. et al.** (2013). BMP signaling controls muscle mass. *Nat. Genet.* **45**, 1309-1318. doi:10.1038/ng.2772
- Schienda, J., Engleka, K. A., Jun, S., Hansen, M. S., Epstein, J. A., Tabin, C. J., Kunkel, L. M. and Kardon, G.** (2006). Somitic origin of limb muscle satellite and side population cells. *Proc. Natl. Acad. Sci. USA* **103**, 945-950. doi:10.1073/pnas.0510164103
- Schuster-Gossler, K., Cordes, R. and Gossler, A.** (2007). Premature myogenic differentiation and depletion of progenitor cells cause severe muscle hypotrophy in Delta1 mutants. *Proc. Natl. Acad. Sci. USA* **104**, 537-542. doi:10.1073/pnas.0608281104
- Seale, P., Sabourin, L. A., Girgis-Gabardo, A., Mansouri, A., Gruss, P. and Rudnicki, M. A.** (2000). Pax7 is required for the specification of myogenic satellite cells. *Cell* **102**, 777-786. doi:10.1016/S0092-8674(00)00666-0
- Silva-Barbosa, S. D., Butler-Browne, G. S., Di Santo, J. P. and Mouly, V.** (2005). Comparative analysis of genetically engineered immunodeficient mouse strains as recipients for human myoblast transplantation. *Cell Transplant.* **14**, 457-467. doi:10.3727/000000005783982837
- Stark, D. A., Karvas, R. M., Siegel, A. L. and Cornelison, D. D. W.** (2011). Eph/ephrin interactions modulate muscle satellite cell motility and patterning. *Development* **138**, 5279-5289. doi:10.1242/dev.068411
- Stark, D. A., Coffey, N. J., Pancoast, H. R., Arnold, L. L., Walker, J. P. D., Vallée, J., Robitaille, R., Garcia, M. L. and Cornelison, D. D. W.** (2015). Ephrin-A3 promotes and maintains slow muscle fiber identity during postnatal development and reinnervation. *J. Cell Biol.* **211**, 1077-1091. doi:10.1083/jcb.201502036
- Tanegashima, K., Suzuki, K., Nakayama, Y., Tsuji, K., Shigenaga, A., Otaka, A. and Hara, T.** (2013a). CXCL14 is a natural inhibitor of the CXCL12-CXCR4 signaling axis. *FEBS Lett.* **587**, 1731-1735. doi:10.1016/j.febslet.2013.04.046
- Tanegashima, K., Tsuji, K., Suzuki, K., Shigenaga, A., Otaka, A. and Hara, T.** (2013b). Dimeric peptides of the C-terminal region of CXCL14 function as CXCL12 inhibitors. *FEBS Lett.* **587**, 3770-3775. doi:10.1016/j.febslet.2013.10.017
- Theret, M., Gsaier, L., Schaffer, B., Juban, G., Ben Larbi, S., Weiss-Gayet, M., Bultot, L., Colodet, C., Foretz, M., Desplanches, D. et al.** (2017). AMPKalpha1-LDH pathway regulates muscle stem cell self-renewal by controlling metabolic homeostasis. *EMBO J.* **36**, 1946-1962. doi:10.15252/embj.201695273

- Thomas, K., Engler, A. J. and Meyer, G. A.** (2015). Extracellular matrix regulation in the muscle satellite cell niche. *Connect. Tissue Res.* **56**, 1-8. doi:10.3109/03008207.2014.947369
- Tierney, M. T. and Sacco, A.** (2016). Satellite cell heterogeneity in skeletal muscle homeostasis. *Trends Cell Biol.* **26**, 434-444. doi:10.1016/j.tcb.2016.02.004
- Urciuolo, A., Quarta, M., Morbidoni, V., Gattazzo, F., Molon, S., Grumati, P., Montemurro, F., Tedesco, F. S., Blaauw, B., Cossu, G. et al.** (2013). Collagen VI regulates satellite cell self-renewal and muscle regeneration. *Nat. Commun.* **4**, 1964. doi:10.1038/ncomms2964
- Vasyutina, E., Stebler, J., Brand-Saberi, B., Schulz, S., Raz, E. and Birchmeier, C.** (2005). CXCR4 and Gab1 cooperate to control the development of migrating muscle progenitor cells. *Genes Dev.* **19**, 2187-2198. doi:10.1101/gad.346205
- Vasyutina, E., Lenhard, D. C., Wende, H., Erdmann, B., Epstein, J. A. and Birchmeier, C.** (2007). RBP-J (Rbpsi) is essential to maintain muscle progenitor cells and to generate satellite cells. *Proc. Natl. Acad. Sci. USA* **104**, 4443-4448. doi:10.1073/pnas.0610647104
- Verma, M., Asakura, Y., Murakonda, B. S. R., Pengo, T., Latroche, C., Chazaud, B., McLoon, L. K. and Asakura, A.** (2018). Muscle satellite cell cross-talk with a vascular niche maintains quiescence via VEGF and notch signaling. *Cell Stem Cell* **23**, 530-543.e539. doi:10.1016/j.stem.2018.09.007
- Wang, H., Noulet, F., Edom-Vovard, F., Tozer, S., Le Grand, F. and Duprez, D.** (2010). Bmp signaling at the tips of skeletal muscles regulates the number of fetal muscle progenitors and satellite cells during development. *Dev. Cell* **18**, 643-654. doi:10.1016/j.devcel.2010.02.008
- Webster, M. T., Manor, U., Lippincott-Schwartz, J. and Fan, C.-M.** (2016). Intravital imaging reveals ghost fibers as architectural units guiding myogenic progenitors during regeneration. *Cell Stem Cell* **18**, 243-252. doi:10.1016/j.stem.2015.11.005
- Welle, S., Cardillo, A., Zanche, M. and Tawil, R.** (2009). Skeletal muscle gene expression after myostatin knockout in mature mice. *Physiol. Genomics* **38**, 342-350. doi:10.1152/physiolgenomics.00054.2009
- White, R. B., Bierinx, A.-S., Gnocchi, V. F. and Zammit, P. S.** (2010). Dynamics of muscle fibre growth during postnatal mouse development. *BMC Dev. Biol.* **10**, 21. doi:10.1186/1471-213X-10-21
- Wosczyzna, M. N. and Rando, T. A.** (2018). A muscle stem cell support group: coordinated cellular responses in muscle regeneration. *Dev. Cell* **46**, 135-143. doi:10.1016/j.devcel.2018.06.018
- Yajima, H. and Kawakami, K.** (2016). Low Six4 and Six5 gene dosage improves dystrophic phenotype and prolongs life span of mdx mice. *Dev. Growth Differ.* **58**, 546-561. doi:10.1111/dgd.12290
- Yajima, H., Motohashi, N., Ono, Y., Sato, S., Ikeda, K., Masuda, S., Yada, E., Kanesaki, H., Miyagoe-Suzuki, Y., Takeda, S. et al.** (2010). Six family genes control the proliferation and differentiation of muscle satellite cells. *Exp. Cell Res.* **316**, 2932-2944. doi:10.1016/j.yexcr.2010.08.001
- Yanagisawa, H., Schluterman, M. K. and Brekken, R. A.** (2009). Fibulin-5, an integrin-binding matricellular protein: its function in development and disease. *J. Cell Commun. Signal.* **3**, 337-347. doi:10.1007/s12079-009-0065-3
- Yin, H., Price, F. and Rudnicki, M. A.** (2013). Satellite cells and the muscle stem cell niche. *Physiol. Rev.* **93**, 23-67. doi:10.1152/physrev.00043.2011
- Zebboudj, A. F., Imura, M. and Boström, K.** (2002). Matrix GLA protein, a regulatory protein for bone morphogenetic protein-2. *J. Biol. Chem.* **277**, 4388-4394. doi:10.1074/jbc.M109683200

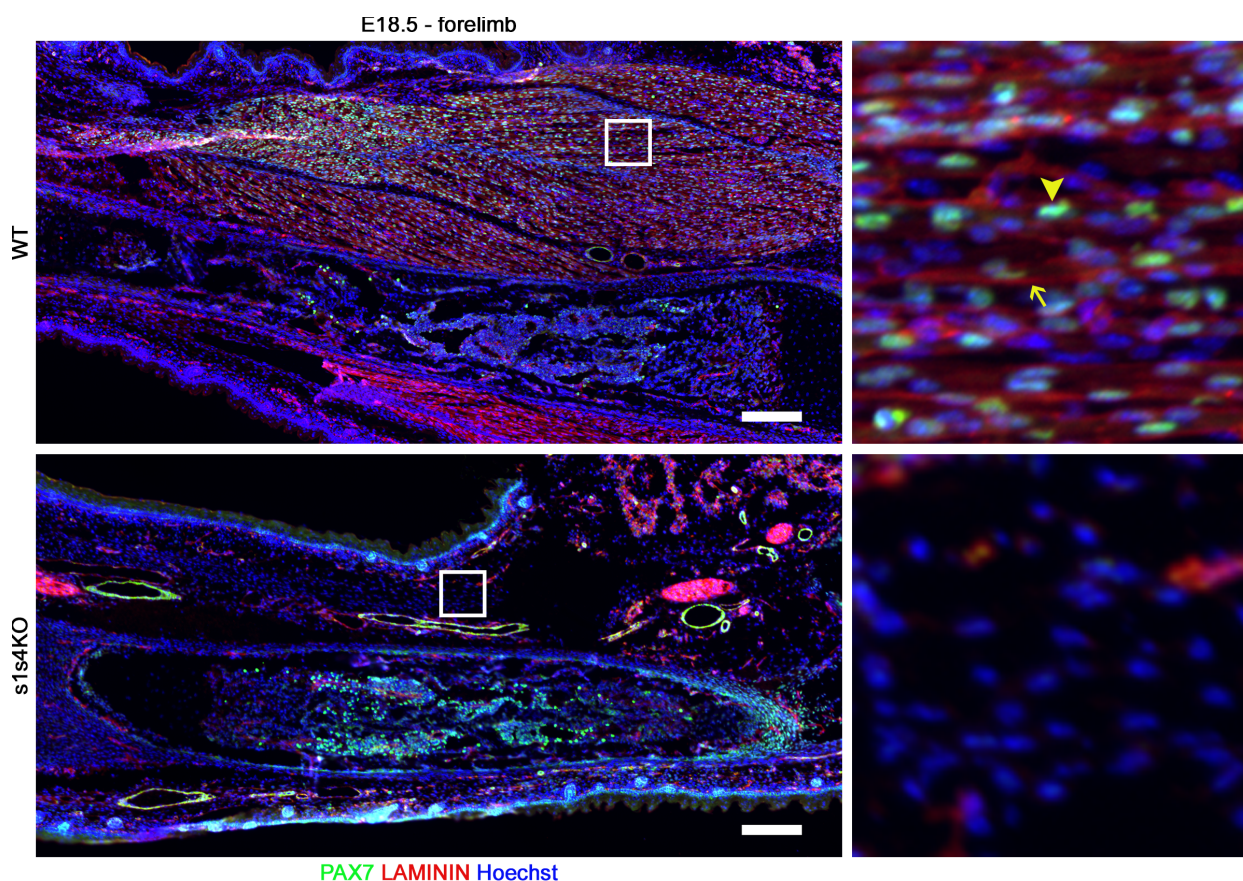


Fig. S1: Six1 and Six4 are required for PAX7+ cell genesis in limb muscles.

Immunostaining for PAX7 (green) and LAMININ (red) on longitudinal sections of E18.5 WT and s1s4KO forelimbs, nuclei stained with Hoechst (blue), sb=200 μ m. Zoom from white squares are shown in the right panels, yellow arrow points to the plasma membrane of a muscle fiber, yellow arrow head points to a PAX7+ cell.

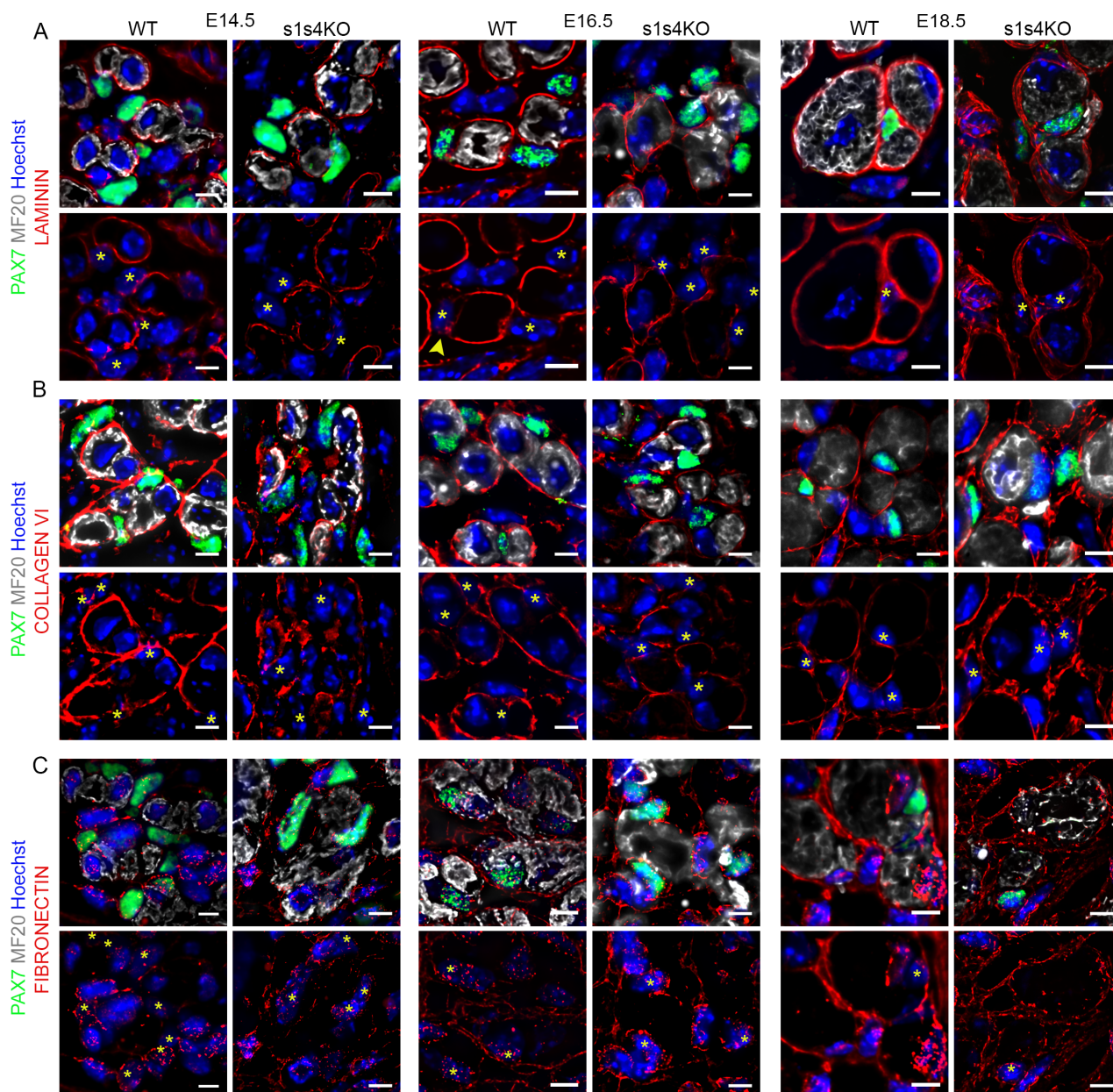


Fig. S2: ECM deposition in WT and s1s4KO fetuses back muscles. Confocal images of immunostainings on E14.5, E16.5 and E18.5 WT or s1s4KO fetuses transversal sections, panels show zoom in epaxial back muscle erector spinae, on all images nuclei are stained with Hoechst (blue), PAX7 is stained in green, an ECM protein is stained in red and Myosins are stained in white. Top panels show merged images of the three stainings and Hoechst and bottom panels only the ECM protein and Hoechst with yellow stars pointing PAX7+ cells, sb=5 μ m. A: Immunostaining for PAX7 (green), LAMININ (red) and MF20 (white). The yellow arrowhead at E16.5 points to a WT PAX7+ cell that seems crossing the basal lamina. B: Immunostaining for PAX7 (green), COLLAGEN VI (red) and MF20 (white). C: Immunostaining for PAX7 (green), FIBRONECTIN (red) and MF20 (white).

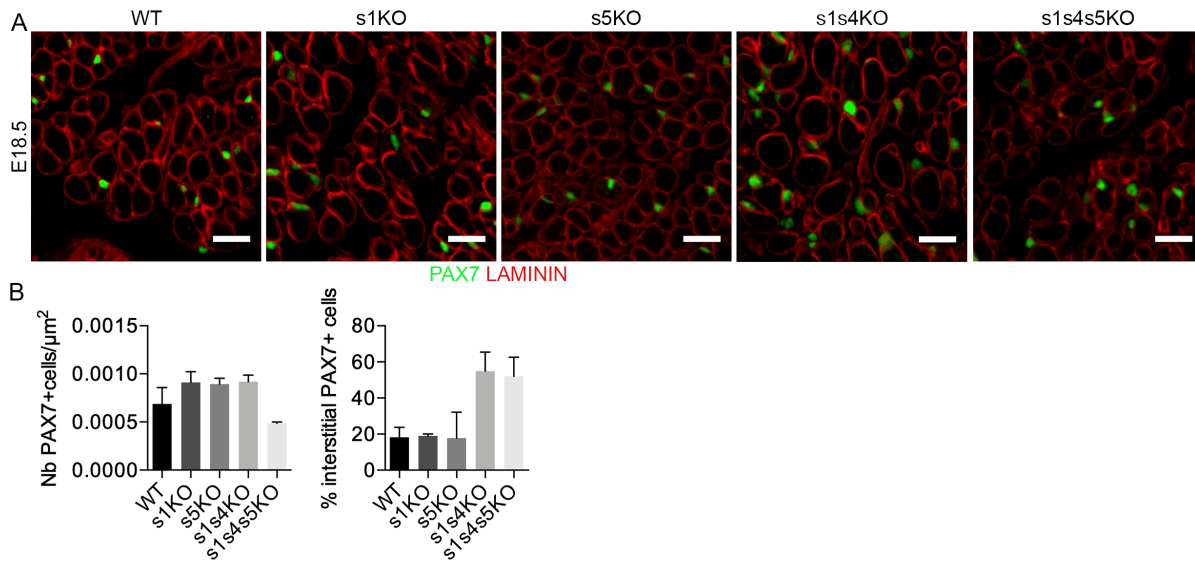


Fig. S3: The homing phenotype is specific of s1s4KO fetuses.

A: Immunostaining for PAX7 (green) and LAMININ (red) on transversal sections of WT, s1KO, s5KO, s1s4KO and s1s4s5KO E18.5 fetuses back muscles, sb=20μm. B: Quantification of the number of PAX7+ cells per μm², WT n=4, s1KO n=2, s5KO n=2, s1s4KO n=2 and s1s4s5KO n=2 and of the percentage of interstitial PAX7+ cells, WT n=6, s1KO n=3, s5KO n=2, s1s4KO n=6 and s1s4s5KO n=2.

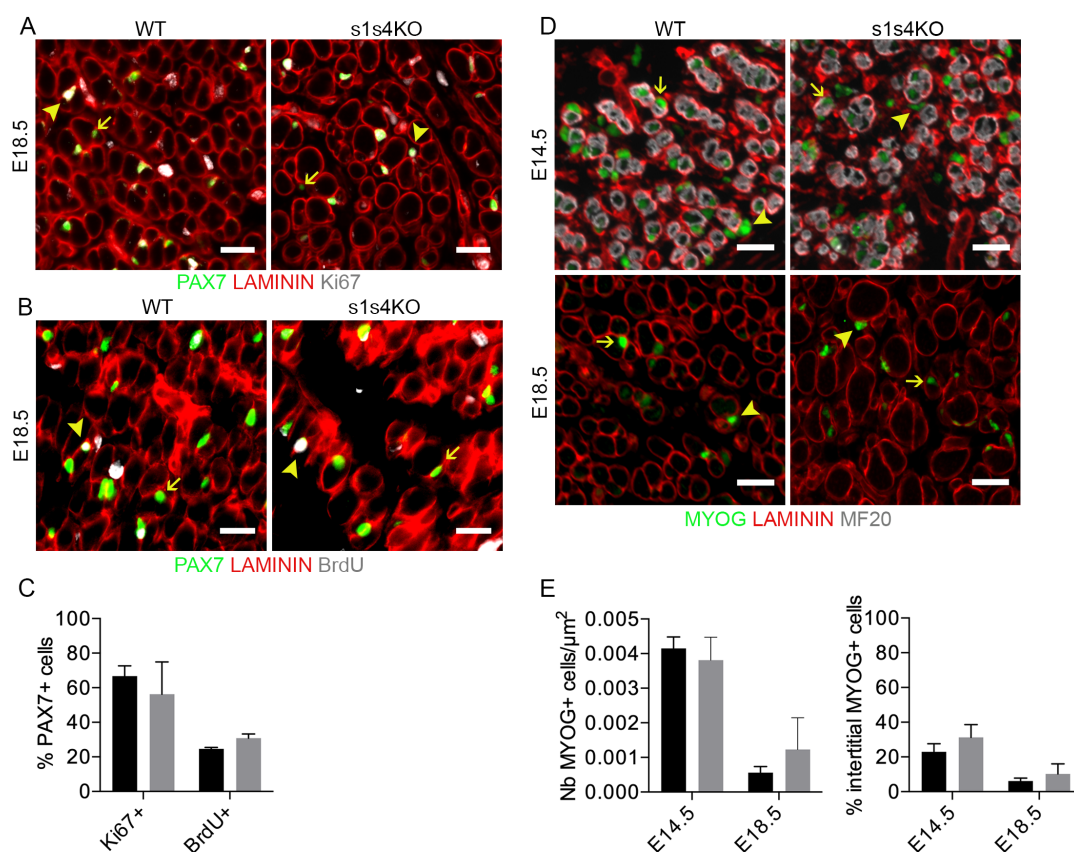


Fig. S4: Mis-localization of s1s4KO PAX7+ cells does not impair their proliferation nor differentiation properties *in vivo*.

A: Immunostaining for PAX7 (green), LAMININ (red) and Ki67 (white) on WT and s1s4KO E18.5 back muscle transversal sections. Arrows point to PAX7+Ki67- cells and arrowheads to PAX7+Ki67+ cells, sb=20μm. B: Immunostaining for PAX7 (green), LAMININ (red) and BrdU (white) on WT and s1s4KO E18.5 back muscle transversal sections. Arrows point to PAX7+BrdU- cells and arrowheads to PAX7+BrdU+ cells, sb=20μm. C: Quantification of the percentage of Ki67+ and BrdU+ cells in the whole PAX7+ cell population in WT and s1s4KO E18.5 fetuses, n=2-3. D: Immunostaining for MYOG (green), LAMININ (red) and MF20 (white, only on E14.5 sections) on WT and s1s4KO E14.5 and E18.5 back muscle transversal sections, sb=20μm. E: Quantification of the number of MYOG+ cells per μm² and of the percentage of interstitial MYOG+ cells in WT and s1s4KO E14.5 and E18.5 back muscles, WT n=3, s1s4KO n=2-3.

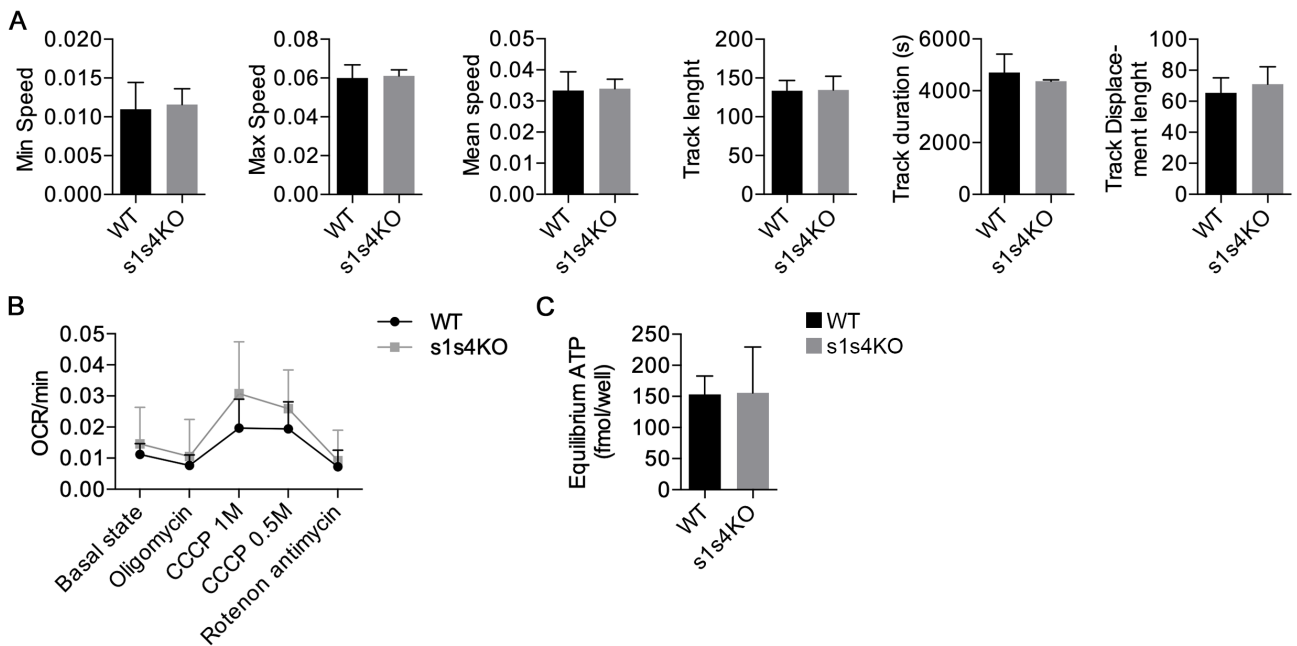


Fig. S5: The absence of Six1 and Six4 expression does not impact migration nor metabolic properties of PAX7+ myoblast *in vitro*.

A: Quantification of the mean, maximum and minimum speed and the duration, length and displacement length of the track of WT and s1s4KO myoblast cultivated on Matrigel and in proliferation medium live imaged for 6 hours, n=3. B: Measure of WT and s1s4KO PAX7+ myoblast oxygen consumption with Seahorse technology, n=3. C: Measure of ATP concentration in WT and s1s4KO PAX7+ myoblasts, n=2.

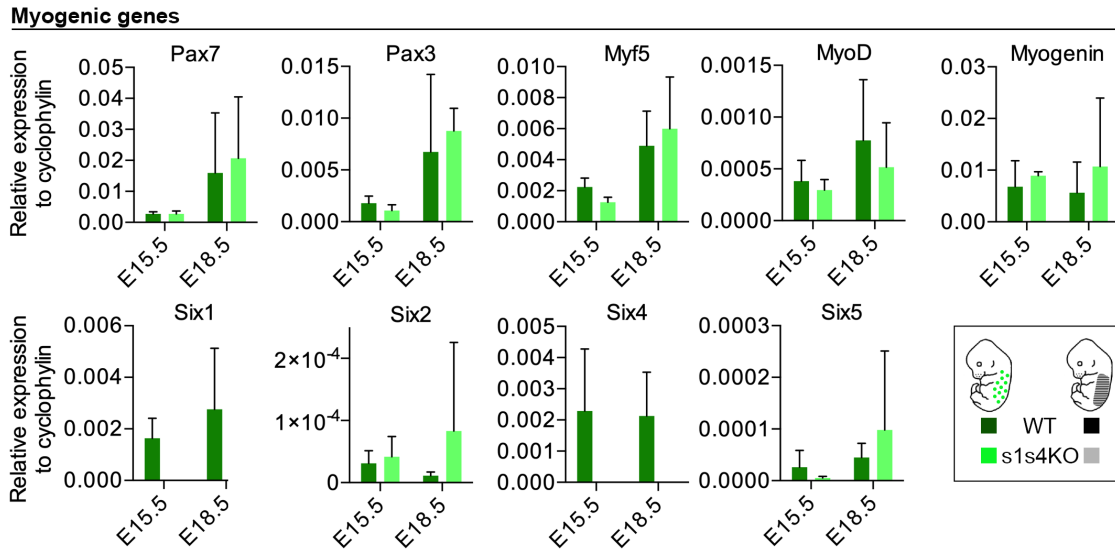


Fig. S6: The absence of *Six1* and *Six4* expression does not alter myogenic gene expression in fetal PAX7+ cells.

qPCR validation of myogenic genes expression in PAX7+ cells (WT dark green, s1s4KO light green) from E15.5 and E18.5 fetuses, n=3.

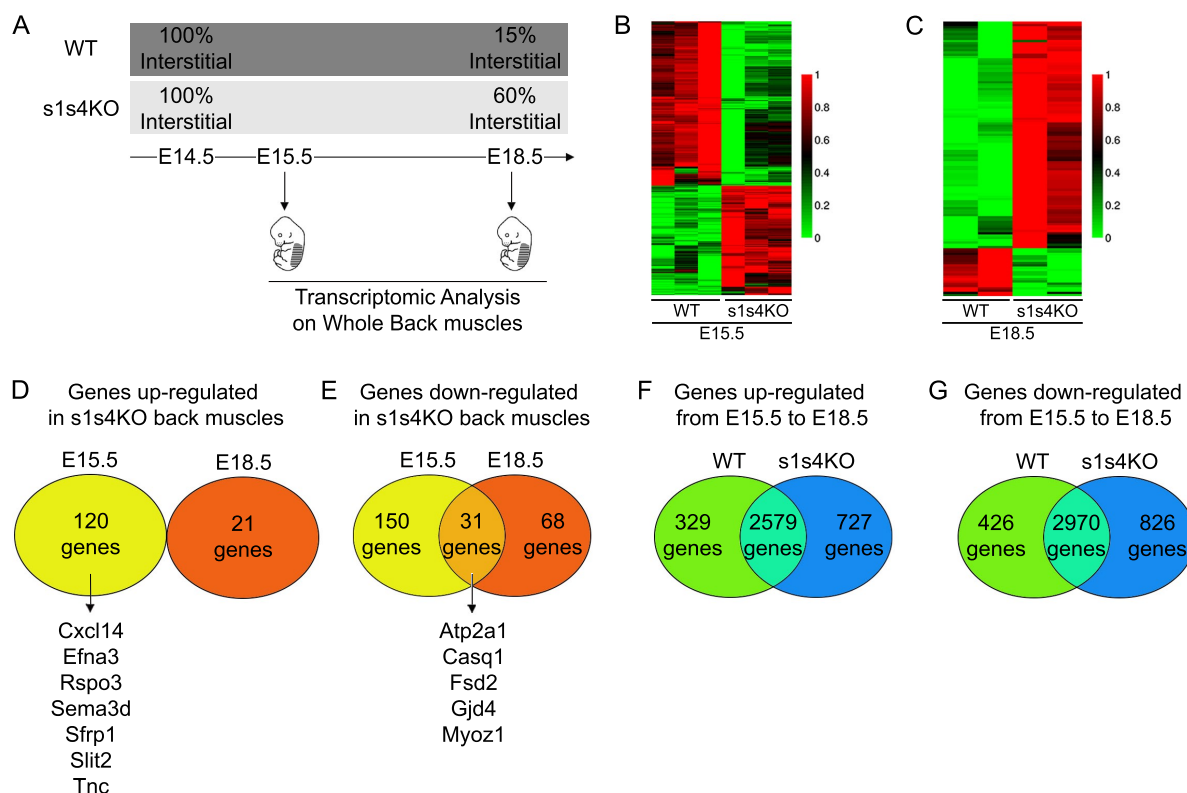


Fig. S7: Transcriptomic analysis of WT and s1s4KO back muscles.

A: Affymetrix analysis has been performed from RNA extracted from the whole back muscles of WT and s1s4KO, E15.5 and E18.5 fetuses. B: Heatmap representing up and down regulated genes between WT and s1s4KO whole back muscles at E15.5. C: Heatmap representing up and down regulated genes between WT and s1s4KO whole back muscles at E18.5. D,E: Venn diagrams representing up-regulated (D) and down-regulated (E) genes in s1s4KO back muscles compared with WT back muscles at E15.5 and E18.5. F,G: Venn diagrams representing up-regulated (F) and down-regulated (G) genes at E18.5 compared with E15.5 WT and s1s4KO back muscles.

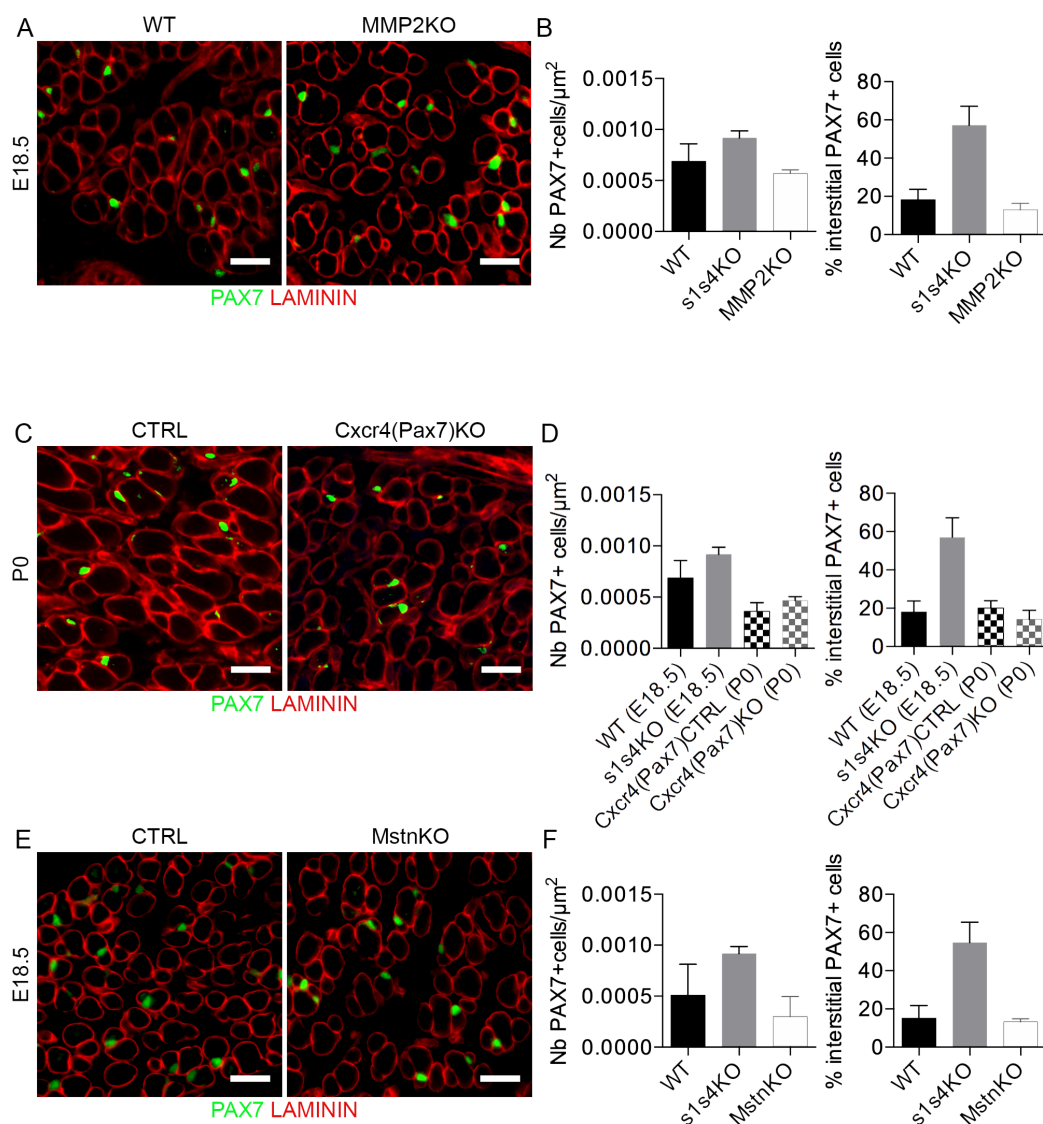


Fig. S8: PAX7+ cell homing is not altered in *Mmp2*, *Cxcr4* nor *Mstn* KO fetuses.

A,C,E: Immunostainings for PAX7 (green) and LAMININ (red) on transversal sections of the back muscles of E18.5 WT and *Mmp2*KO fetuses (A), P0 CTRL and *Cxcr4* conditional KO in *Pax7* expressing cells (*Cxcr4*(*Pax7*)KO) new born mice (C), WT and *Mstn* KO E18.5 fetuses (E). B,D,F: Quantification of the number of PAX7+ cells per μm² and the percentage of interstitial PAX7+ cells in the back muscles of E18.5 WT, s1s4KO and *Mmp2* KO n=2 (B), of P0 CTRL and *Cxcr4*(*Pax7*)KO new born mice, n=2 (D), of WT, s1s4KO and *Mstn* KO E18.5 fetuses, n=2-3 (F). In all panels sb=20 μm.

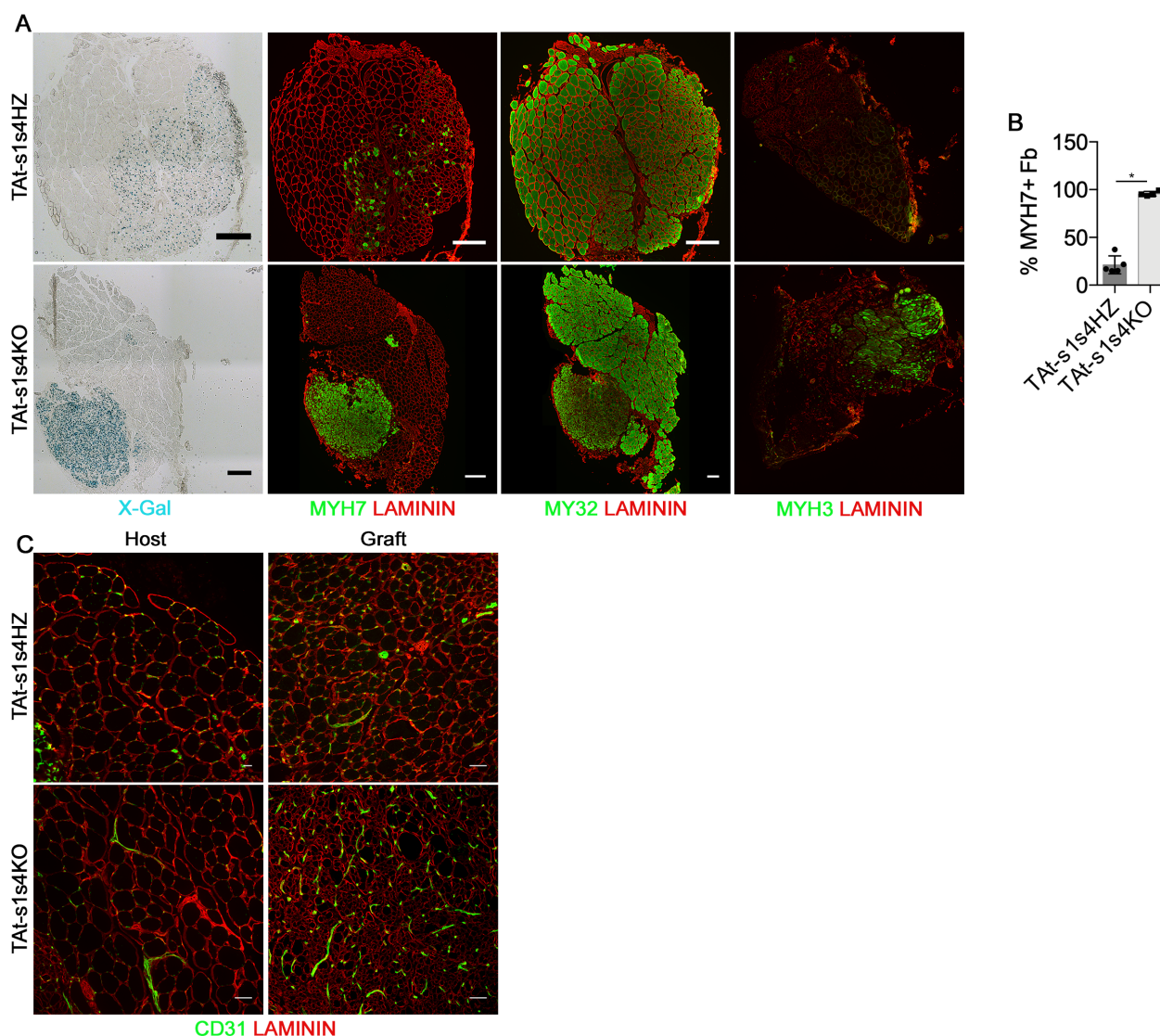


Fig. S9: Transplanted s1s4KO PAX7+ cells only produce MYH7+ fibers with no obvious impact on vascularization.

A: XGal staining of Six1-LacZ+ cells, immunostaining for MYH7, MY32 or MYH3 (green) and LAMININ (red) on whole muscle sections of TA transplanted with s1s4HZ or s1s4KO PAX7+ cells, sb=300µm. B: Quantification of the percentage of MYH7+ fibers in the graft region of TA transplanted with s1s4HZ (n=4-5) or s1s4KO (n=3) PAX7GFP+ cells, * pvalue<0.05. C: Immunostaining for CD31 (green) and LAMININ (red) in the host and graft regions of TA muscles transplanted with s1s4HZ or s1s4KO PAX7+ cells, sb=50µm.

Table S1: Up-regulated genes in s1s4KO PAX7+ cells (PAX7_UP_WTvsKO) List of the 22 genes exclusively up-regulated at E15.5, 114 genes exclusively up-regulated at E18.5 and 1 gene up-regulated at both E15.5 and E18.5 in s1S4KO PAX7+ cells. This include genes with fold-change (FC) > 2 and ANOVA p-value < 0.05.

[Click here to Download Table S1](#)

Table S2: Down-regulated genes in s1s4KO PAX7+ cells (PAX7_DOWN_WTvsKO)

List of the 31 genes exclusively down-regulated at E15.5, 101 genes exclusively down-regulated at E18.5 and 6 genes down-regulated at both E15.5 and E18.5 in s1S4KO PAX7+ cells. This include genes with fold-change (FC) < -2 and ANOVA p-value < 0.05.

[Click here to Download Table S2](#)

Table S3: Up-regulated genes at E18.5 compared to E15.5 PAX7+ cells (Pax7_UP_E18vsE15)

List of the 234 genes exclusively up-regulated in WT PAX7+ cells, 104 genes exclusively up-regulated in s1s4KO PAX7+ cells and 132 genes up-regulated in both WT and s1S4KO PAX7+ cells. This include genes with fold-change (FC) > 2 and ANOVA p-value < 0.05.

[Click here to Download Table S3](#)

Table S4: Down-regulated genes at E18.5 compared to E15.5 PAX7+ cells (PAX7_DOWN_E18vsE15)

List of the 427 genes exclusively down-regulated at in WT PAX7+ cells, 218 genes exclusively down-regulated s1s4KO PAX7+ cells and 121 genes down-regulated in both WT and s1S4KO PAX7+ cells. This include genes with fold-change (FC) < -2 and ANOVA p-value < 0.05.

[Click here to Download Table S4](#)

Table S5: Up-regulated genes in s1s4KO whole back muscles (Muscle_UP_WTvsKO)

List of the 120 genes exclusively up-regulated at E15.5 and 21 genes exclusively up-regulated at E18.5 in s1S4KO back muscles. This include genes with fold-change (FC) > 2 and ANOVA p-value < 0.05.

[Click here to Download Table S5](#)

Table S6: Down-regulated genes in s1s4KO whole back muscles (Muscle_DOWN_WTvsKO)

List of the 150 genes exclusively down-regulated at E15.5, 68 genes exclusively down-regulated at E18.5 and 31 genes down-regulated at both E15.5 and E18.5 in s1S4KO back muscles. This include genes with fold-change (FC) < -2 and ANOVA p-value < 0.05.

[Click here to Download Table S6](#)

Table S7: Up-regulated genes at E18.5 compared to E15.5 whole back muscles (Muscle_UP_E18vsE15)

List of the 329 genes exclusively up-regulated in WT back muscles, 727 genes exclusively up-regulated in s1s4KO back muscles and 2579 genes up-regulated in both WT and s1s4KO back muscles. This include genes with fold-change (FC) > 2 and ANOVA p-value < 0.05.

[Click here to Download Table S7](#)

Table S8: Down-regulated genes at E18.5 compared to E15.5 whole back muscles (Muscle_DOWN_E18vsE15)

List of the 426 genes exclusively down-regulated at in WT back muscles, 826 genes exclusively down-regulated in s1s4KO back muscles and 2970 genes down-regulated in both WT and s1s4KO back muscles. This include genes with fold-change (FC) < -2 and ANOVA p-value < 0.05.

[Click here to Download Table S8](#)

Table S9: Gene of interest in PAX7+ FACS-sorted cells

List of the genes of interest and their respective FC and p-value values from the ANOVA analysis of Affymetrix data comparing WT and s1s4KO PAX7+ cells at E15.5 and E18.5.

[Click here to Download Table S9](#)

Table S10: Gene of interest in whole back muscles

List of the genes of interest and their respective FC and p-value values from the ANOVA analysis of Affymetrix data comparing WT and s1s4KO whole back muscles at E15.5 and E18.5.

[Click here to Download Table S10](#)

Table S11: Expression values in PAX7+ FACS-sorted cells

List of the expression of all genes in WT and s1s4KO PAX7+ cells at E15.5 and E18.5.

[Click here to Download Table S11](#)

Table S12: Expression values in whole back muscles

List of the expression of all genes in WT and s1s4KO whole back muscles at E15.5 and E18.5.

[Click here to Download Table S12](#)

Table S13: Antibodies table

List of antibodies used in our study, with target protein name, species of production, company, reference, dilution used and protocol referring to the method section.

[Click here to Download Table S13](#)

Table S14: Oligonucleotide sequences table

Oligonucleotide sequences used for RTqPCR analysis.

[Click here to Download Table S14](#)